Drainage network development in the Keanakāko‘i tephra, Kīlauea Volcano, Hawai‘i: Implications for fluvial erosion and valley network formation on early Mars

Robert A. Craddock,[1] Alan D. Howard,[2] Rossman P. Irwin III,[1] Stephen Tooth,[3] Rebecca M. E. Williams,[4] and Pao-Shin Chu[5]

Received 1 March 2012; revised 11 June 2012; accepted 4 July 2012; published 22 August 2012.

[1] A number of studies have attempted to characterize Martian valley and channel networks. To date, however, little attention has been paid to the role of lithology, which could influence the rate of incision, morphology, and hydrology as well as the characteristics of transported materials. Here, we present an analysis of the physical and hydrologic characteristics of drainage networks (gullies and channels) that have incised the Keanakāko‘i tephra, a basaltic pyroclastic deposit that occurs mainly in the summit area of Kīlauea Volcano and in the adjoining Ka‘ū Desert, Hawai‘i. The Keanakāko‘i tephra is up to ~10 m meters thick and largely devoid of vegetation, making it a good analog for the Martian surface. Although the scales are different, the Keanakāko‘i drainage networks suggest that several typical morphologic characteristics of Martian valley networks may be controlled by lithology in combination with ephemeral flood characteristics. Many gully headwalls and knickpoints within the drainage networks are amphitheater shaped, which results from strong-over-weak stratigraphy. Beds of fine ash, commonly bearing accretionary lapilli (pisolites), are more resistant to erosion than the interbedded, coarser weakly consolidated and friable tephra layers. Because the banks of the gullies and channels are easily eroded widths vary downslope, similar to Martian valley networks that have been characterized as “degraded.” The floors of the gullies and channels tend to be low-relief with few prominent bed forms, reflecting the large proportion of sediment transported as bed load in high-energy but short-lived flood events. We calculate that the average flow velocities within the drainage networks are typically <10 cm/s, occurring during floods that probably last less than an hour. Analyses of sediment deposits that have overlain lava flows of known ages suggest that these ephemeral flood events are associated with large cold core winter cyclones, known locally as ‘kona storms’, that are capable of generating precipitation at rates >1 m/24 h. Given some recent modeling of the early Martian climate, our observations imply that rainfall on early Mars could also be associated with large intense events and that Martian valley network formation may be related to similar cyclonic storms.

Citation: Craddock, R. A., A. D. Howard, R. P. Irwin III, S. Tooth, R. M. E. Williams, and P.-S. Chu (2012), Drainage network development in the Keanakāko‘i tephra, Kīlauea Volcano, Hawai‘i: Implications for fluvial erosion and valley network formation on early Mars, *J. Geophys. Res.*, *117*, E08009, doi:10.1029/2012JE004074.

[1]Center for Earth and Planetary Studies, National Air and Space Museum, Smithsonian Institution, Washington, DC, USA.
[2]Department of Environmental Sciences, University of Virginia, Charlottesville, Virginia, USA.
[3]Institute of Geography and Earth Sciences, Aberystwyth University, Aberystwyth, UK.
[4]Planetary Science Institute, Tucson, Arizona, USA.
[5]Department of Meteorology, University of Hawai‘i at Manoa, Honolulu, Hawai‘i, USA.

Corresponding author: R. A. Craddock, Center for Earth and Planetary Studies, National Air and Space Museum, MRC-315, Smithsonian Institution, Washington, DC 20560, USA. (craddockb@si.edu)

1. Introduction

[2] Valley networks are thought to be the best evidence that liquid water was once present on the Martian surface [e.g., *Carr*, 1996]. Numerous studies have mapped their location [e.g., *Hoke and Hynek*, 2009] or attempted to quantify their various characteristics [e.g., *Irwin et al.*, 2011] in an effort to better understand when valley networks were active, how long they were active, and the processes involved in their formation. To date, however, little attention has been paid to the possible role of lithology in the formation of Martian valley networks. Studies of terrestrial valley, channel, and gully development have shown that catchment lithology can influence surface runoff characteristics, incision rates,

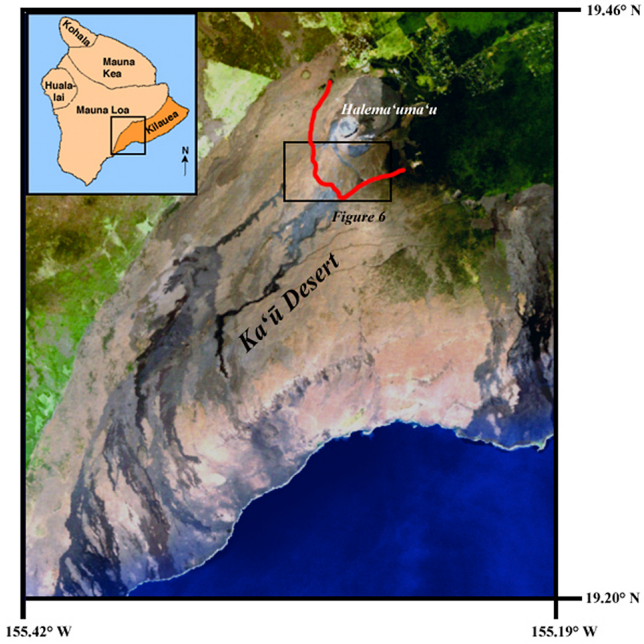

Figure 1. GEX image showing the location of the study area with respect to the Big Island of Hawai'i and the five major volcanoes (inset). The red line shows the extent of the continuous deposit of the Keanakāko'i tephra as mapped by *Malin et al.* [1983] (their unit 1). The location of Figure 6 is also shown for reference.

morphological development, and the characteristics of transported materials [e.g., *Leopold et al.*, 1992]. It is not possible to say exactly what the lithology of the Martian surface might be at any particular location, especially at depth, or how it may have been different in the past, but there is clear evidence from both lander [*Squyres et al.*, 2004] and orbital data [*Bandfield et al.*, 2000] that most of the surface is basaltic in composition, and most likely brecciated due to impact cratering or volcanism. Many highland intercrater plains and basin-fill materials are visibly stratified [*Malin and Edgett*, 2000]. Few places on Earth share all of these characteristics over extensive areas (>100 km^2), but one notable exception is the Keanakāko'i tephra, a basaltic pyroclastic deposit that occurs mainly in the summit area of Kīlauea Volcano and in the adjoining Ka'ū Desert, Hawai'i (Figure 1).

[3] Here we present an analysis of drainage network development in the Keanakāko'i tephra to address the possible influences of lithology on Martian valley network development. Despite the difference in scales, the drainage networks that have incised the Keanakāko'i tephra share many of the same morphologic characteristics as Martian valley networks, including amphitheater-shaped headwalls and knickpoints, variable widths downslope, and low-relief floors. While such characteristics are often attributed to formation by groundwater sapping [e.g., *Goldspiel et al.*, 1993], we show that sapping plays no role in the development of drainage networks in the Keanakāko'i. Instead, morphology is controlled by a combination of lithology and ephemeral flood events. For example, the bank strength of the Keanakāko'i tephra is inherently weak due to the poorly consolidated nature of much of the tephra, so bank erosion can occur easily during flooding. Thus, in planform the width of the gullies and channels varies extensively and independently of slope length, which is similar to Martian valley networks that have been described as "degraded" [*Baker and Partridge*, 1986; *Gulick*, 2001; *Hoke and Hynek*, 2009]. Although the Ka'ū Desert receives ~130 cm (~50 inches) of rainfall annually [*Giambelluca and Sanderson*, 1993] flow through the drainage networks is ephemeral, and erosion and sediment transport appear to be associated primarily with large kona storms, which are cold core cyclones that occur in the Pacific during the winter months. Recent climatic models indicate that similar cyclones may have formed early in Martian history if an ocean in the northern hemisphere was present [*Richardson and Soto*, 2008]. The implications of our study are that the morphology of many Martian valley networks may be strongly influenced by local lithology and that large, slow-moving storms capable of delivering precipitation at rates of tens to hundreds of centimeters a day may have been necessary to generate the runoff necessary to carve the valley networks.

2. Background

2.1. Nature of the Martian Surface

[4] It is clear from geologic features such as the Tharsis volcanoes [e.g., *Carr*, 1973], analyses of the Shergottites/Nakhlites/Chassignites (SNC) meteorites [e.g., *McSween*, 1994], multispectral data from orbiting spacecraft [e.g., *Bandfield et al.*, 2000], and in situ measurements made by landers [e.g., *Gellert et al.*, 2004] that the Martian surface is composed primarily of basalt. For decades we have also had an appreciation that most of this basaltic surface has been broken down into friable materials due to weathering, impact cratering and explosive volcanism [*Soderblom et al.*, 1973; *Binder et al.*, 1977; *Mutch et al.*, 1977]. The generally accepted initial paradigm was that Mars had a brecciated regolith that was superposed by ejecta or dust mantles in places [e.g., *Fanale and Cannon*, 1971]. This thinking was influenced by our experience during the Apollo era, but as our understanding of Mars has deepened the evidence suggests that this paradigm is a bit too simplistic, and there is now clearer evidence of the relative roles of different geologic processes in constructing the landscape preserved today. *Malin and Edgett* [2001], for example, present evidence suggesting that extensive weathering, transport and deposition during the first billion years of Martian history created a layered terrain up to depths of several kilometers. Some of these layers may represent tephra deposits emplaced by volcanic eruptions [*Edgett and Malin*, 2000, 2002]. In fact, the possibility that there are widespread tephra deposits on Mars has recently gained additional credibility, as data obtained by the Spirit Mars Exploration Rover shows evidence for well-expressed, fine-scale layering, which may have been produced by explosive volcanism [*Squyres et al.*, 2007]. There is also evidence that explosive volcanism preceded the formation of Hrad [*Wilson and Mouginis-Mark*, 2003] and Mangala Valles [*Wilson and Head*, 2004]. Because current atmospheric pressures are so low on Mars even a small amount of volatiles within the magma should cause lavas to erupt explosively [*Fagents and Wilson*, 1996; *Wilson*, 1999; *Head and Wilson*, 2002]. As a result, ash and tephra deposits should be common, particularly in younger units due to the putative decrease in atmospheric pressure

that may have occurred since the Hesperian [e.g., *Craddock and Howard*, 2002]. This is not to say that explosive volcanic deposits are ubiquitous, but spacecraft data are beginning to reveal the importance of phreatomagmatic eruptions as a basic geologic process on Mars [*Malin and Edgett*, 2001; *Edgett and Malin*, 2002; *Manga et al.*, 2012].

[5] In addition to volcanic processes, *Irwin and Howard* [2002] showed that impact cratering and fluvial erosion were simultaneous processes that competed with one another for surface area early in Martian history, and *Craddock and Howard* [2002] showed that crater modification was a long-lived process that continued as new craters formed. Over time this complex combination of geologic processes could have resulted in a layered landscape containing brecciated and fluvially reworked sediments [*Malin and Edgett*, 2001; *Edgett and Malin*, 2002]. Given that layered, brecciated basaltic material can describe much of the Martian surface, we can assess the environmental conditions necessary to generate runoff and initiate fluvial erosion on such a surface using the Keanakāko'i tephra as an analog.

2.2. Martian Valley Networks

[6] A number of studies have characterized Martian valley networks. The locations of valley networks have been determined several ways, including mapping from imagery data [e.g., *Hynek et al.*, 2010] and by applying computer algorithms to available topographic data to extract watershed information [e.g., *Mest and Crown*, 2008; *Luo and Stepinski*, 2009; *Mest et al.*, 2010]. Although there is some contention about the reliability of both methods, two observations are clear. First, Martian valley networks are located predominantly in the southern cratered highlands, particularly in the equatorial regions between latitudes of $\pm 30^{\circ}$ [*Luo and Stepinski*, 2009; *Hoke and Hynek*, 2009]. There are notable exceptions, however, including valley networks on the Tharsis volcanoes, particularly Alba Patera [e.g., *Ivanov and Head*, 2006], as well as in scattered locations around Valles Marineris [*Williams and Malin*, 2004; *Mangold et al.*, 2004]. Nonetheless, the fact that valley networks are preferentially located in the equatorial regions has led many investigators to suggest that there is a relation to a past climate that may have supported precipitation and surface runoff [*Masursky et al.*, 1977; *Craddock and Maxwell*, 1993; *Craddock and Howard*, 2002; *Harrison and Grimm*, 2005; *Irwin et al.*, 2005a; *Luo and Stepinski*, 2009; *Hoke and Hynek*, 2009; *Hynek et al.*, 2010]. Second, valley networks frequently lack smaller, lower order, space-filling tributaries. Thus, their drainage densities are often lower than most terrestrial drainage systems when compared at the same scale [*Mest and Crown*, 2008; *Luo and Stepinski*, 2009; *Hynek et al.*, 2010], although these densities are certainly not several orders of magnitude lower as was previously believed from Viking Orbiter analyses [*Carr and Chuang*, 1997]. Whether lower Martian drainage densities are a function of preservation, the requirement for larger contribution areas to initiate erosion under lower gravity conditions, an issue of "maturity" (i.e., duration of fluvial erosion), high infiltration capacity relative to precipitation, or some combination of these factors remains unclear.

[7] Chronologic control for valley networks is difficult to establish because they are small, linear features that can easily be modified or destroyed by impact cratering. However, several techniques for age estimation have been developed, including 1) the "buffered crater counting technique" that counts the number of craters that occur around the margin of the valley networks [*Fassett and Head*, 2008a; *Hoke and Hynek*, 2009]; 2) the "high resolution dating technique" that counts smaller diameter craters that occur on the floors of the valley networks [*Quantin and Craddock*, 2008]; and 3) the "basin technique" that counts the craters that occur in the drainage basins associated with the valley networks [e.g., *Ansan and Mangold*, 2006]. Although the different techniques can be helpful in determining the timing and extent of local resurfacing [*Bouley et al.*, 2010], in general a vast majority of the valley networks located in the cratered highlands are early Hesperian in age or older, suggesting that valley network formation declined around the Noachian/Hesperian boundary [*Fassett and Head*, 2008a; *Hoke and Hynek*, 2009; *Bouley et al.*, 2010]. Unfortunately, crater-derived age estimates can only tell when valley network development ceased and the surfaces became stable. It is not possible to determine when valley network formation began, but there is some evidence that it was confined to a "climatic optimum" that began sometime during the late Noachian. This evidence is indirect, however, and is based on the observation that valley network drainage networks are not well integrated [*Irwin et al.*, 2005a; *Fassett and Head*, 2008b]. Essentially, given enough time valley networks should have incised into impact craters, filling them with water until they overflowed and were breached on the other side. This did not occur widely, however, and breached craters are relatively rare [*Irwin et al.*, 2005a; *Fassett and Head*, 2008b], indicating that valley network formation did not occur throughout the entire Noachian [*Irwin et al.*, 2005a].

[8] *Baker and Partridge* [1986] described two distinct morphologic classes of valley networks. "Degraded" valleys have flat-floors and amphitheater-shaped headwalls with "eroded sides," whereas "pristine" valley networks have steep sides and V-shaped cross-sectional profiles. They observed "pristine" valley networks downstream of "degraded" valley networks, and suggested that following their formation many valley networks underwent extensive modification. Subsequently, they were partially reactivated by a later fluvial episode. Because "degraded" valley networks typically share most of their morphologic characteristics with terrestrial valleys and channels argued to have been formed by groundwater sapping [e.g., *Laity and Malin*, 1985], many early investigators suggested that Martian valley networks also formed primarily by groundwater sapping [*Pieri*, 1980; *Baker and Partridge*, 1986; *Goldspiel et al.*, 1993; *Squyres and Kasting*, 1994; *Gulick*, 2001]. However, analyses of Mars Orbiter Laser Altimeter (MOLA) data indicate the opposite spatial relationship, namely that V-shaped valley networks are typically located upstream of valley networks with flat floors [*Williams and Phillips*, 2001; *Carr*, 2006, p. 132], which is more typical of actively eroding fluvial systems [e.g., *Craddock and Howard*, 2002].

[9] This brings up a discussion of terminology. A channel represents the physical confines of a river or stream and consists of banks and a bed. The flow of water and movement of sediment control the development of a channel. In contradistinction, a valley is the broader topographic depression eroded over time by a river or stream. In non-glaciated areas, a valley will tend to be V-shaped upstream where the gradient

is steep and the river is actively eroding. Down-valley, as the gradient becomes shallower and contributing area increases, the valley floor tends to broaden, and ultimately valley floor width will greatly exceed river width, typically resulting in floodplain development. Basically, valley networks represent former river valleys, but are not river channels per se. Although they are rarely preserved, *Irwin et al.* [2005b] have identified a number of former channels within valley networks using high-resolution images. The flat-floor morphology of many valley networks has been used to argue that they were formed by groundwater sapping, but as we discuss below there is nothing unique about this physical characteristic as many terrestrial drainage networks formed by rainfall and surface runoff can also have low-relief floors, including the gullies and channels that have incised into the Keanakāko‘i tephra.

2.3. Keanakāko‘i Tephra

[10] Kīlauea is an active basaltic volcano that constitutes the southeastern portion of the island of Hawai‘i. The ~350 km^2 Ka‘ū Desert is situated southwest of the summit of Kīlauea and is bounded approximately by Hawai‘i State Highway 11 to the west, the National Park Service’s Hilina Pali Road to the east, Kīlauea’s summit caldera to the north, and the Pacific Ocean to the south (Figure 1). Typically, the area receives ~130 cm (~50 inches) of rain every year [*Giambelluca and Sanderson*, 1993], so the Ka‘ū Desert is not a true desert but rather is semi-arid region based on *Meigs*’ [1953] classification. However, the Ka‘ū Desert is almost devoid of any vegetation except along its borders, primarily because of acid fog or rain formed in the SO_2-rich outgassing from Kīlauea’s central pit caldera, Halema‘uma‘u, as well as adjacent fumaroles located in Kīlauea’s summit caldera. On average, Kīlauea outgases over 4.15×10^5 tons of SO_2 every year [*Elias et al.*, 1998], and the trade winds carry these gasses into the desert, contributing to the harsh, acidic conditions that severely limit plant life.

[11] The Keanakāko‘i tephra is the primary source of all basaltic sedimentary material found in the Ka‘ū Desert. This basaltic pyroclastic deposit includes all fragmental deposits emplaced during explosive eruptions from the summit caldera of Kīlauea between ca. 1500 and 1823 AD [*Swanson et al.*, 2012]. The Keanakāko‘i tephra is more than 10 m thick [*McPhie et al.*, 1990; *Swanson et al.*, 2012] in cliffs along the southern margin of the caldera west of Keanakāko‘i Crater, but it thins from there in all directions. The Keanakāko‘i tephra records many different eruptions; the timing, duration, and nature of these eruptions have been the subject of contention, primarily because disconformities within the formation have been interpreted differently [*McPhie et al.*, 1990; *Swanson et al.*, 2012]. A full discussion of these competing interpretations is beyond the scope of this manuscript, but most investigators agree on some general characteristics. Two principal lithologic units are easily distinguishable in most exposures. The upper unit consists mainly of lithic ash and blocks emplaced by pyroclastic density currents and falls. Fine-grained ash layers that are rich in accretionary lapilli occur as interbeds between layers of coarser-grained ash. Sieve analyses show that this unit is moderately to poorly sorted (σ = 1.0) and coarsely skewed ($Sk = -0.25$) with blocks that can sometimes be a few tens of centimeters in size. Typically, however, the particles are <4 mm (pebbles) to 0.25 mm (sand) in size. The lower unit consists of mostly vitric ash and pumice, has a slight greenish-gold color, and results mainly from pyroclastic falls and lesser density currents. Although layers are apparent within this unit, cross bedding is rare. In contrast to the upper unit, sieve analyses show that the lower unit is generally well sorted (σ = 0.45) and nearly symmetrical ($Sk = -0.02$) with particles that are typically 0.25 to 0.75 mm in size (fine to coarse sand). Figure 2 provides an example of what an outcrop of Keanakāko‘i tephra looks like in the field.

[12] Noting these distinct differences between the upper and lower units, *Powers* [1916] suggested that phreatomagmatic eruptions at Kīlauea took place during two separate periods: the upper, lithic unit was emplaced during a large eruption that was witnessed by westerners in 1790, and the lower, vitric unit was emplaced during prehistoric times. *Stone* [1926] and *Wentworth* [1938] suggested that the older section was emplaced 300–500 years ago, but *Powers* [1948] suggested that the entire formation had been emplaced over a longer period of ~1500 years.

[13] In the 1980s, the generally accepted interpretation was that the Keanakāko‘i tephra was emplaced entirely during the 1790 eruption [*Decker and Christiansen*, 1984; *Malin et al.*, 1983; *Easton*, 1987]. In particular relevance to our analyses, *Decker and Christiansen* [1984] noted that a “careful search has revealed no clear evidence of stream erosion, channel gravel, or soil formation within the Keanakāko‘i section,” which otherwise would have indicated that there were multiple eruption episodes. Such an assertion is untenable, however, as there is, in fact, clear evidence for at least two older erosional surfaces [*McPhie et al.*, 1990; *Mastin*, 1997], particularly between the upper lithic unit and the lower vitric unit (e.g., Figure 3). Additionally, the physical characteristics of the deposits record dramatic changes in eruption styles, and isopach maps of the deposits show variations in how the tephra was dispersed during emplacement [*McPhie et al.*, 1990].

[14] Based on ^{14}C ages of charcoal collected from the base of the Keanakāko‘i tephra, *Swanson et al.* [2004, 2012] estimated that explosive eruptions and tephra emplacement began about 1470–1490 AD. However, including evidence from the older Kulanaokuaiki tephra [*Fiske et al.*, 2009] and the Uwekahuna ash, the current belief is that Kīlauea has experienced periodic phreatomagmatic eruptions for at least the last 2000–3000 years [*Dzurisin et al.*, 1995]. It is interesting to note that despite Kīlauea’s reputation for quiescent eruptions, the phreatomagmatic eruption that took place in 1790 killed a war party of at least 80 Hawaiians, giving Kīlauea the distinction as the deadliest volcano in America [*Swanson and Christiansen*, 1973]. There are probably multiple reasons why Kīlauea erupts explosively. Until recently, the last explosive eruption took place in 1924 when the floor of Halema‘uma‘u quickly withdrew to a depth of over 400 m within a period of a few weeks [*Decker and Christiansen*, 1984]. In this instance, an offshore eruption caused the caldera floor to sink below the water table [*McPhie et al.*, 1990; *Mastin*, 1997]. This movement subsequently triggered a phreatomagmatic eruption that emplaced small amounts of ash and blocks near the summit. Another small phreatomagmatic eruption began in March 2008 [*Wilson et al.*, 2008]. A large lava lake situated a few tens of meters below Halema‘uma‘u drives the ongoing eruption.

Figure 2. A close-up of the Keanakāko‘i tephra showing the disconformity between the upper, lithic-rich unit, which is purplish in color, and the lower, vitric-rich unit, which is greenish-gold in color. Note also the difference in grain-sizes and sorting between the two units. The upper unit is poorly sorted and contains particles that can be tens of centimeters in size. Typically, however, the particles are <4 mm (pebbles) to 0.25 mm (sand) in size. Also note the occurrence of lapilli-rich ash layers. The lower unit consists of mostly vitric ash and pumice that is well sorted with particles that are typically 0.25 to 0.75 mm in size (fine to coarse sand). The physical differences between the two units affects the competency of the units and their resistance to erosion. The researcher is pointing to the margin of a small gully that incised the lower unit prior to the emplacement of the upper unit.

Outgassing from this lava lake escapes through a vent in the caldera floor, which periodically collapses, enlarging the vent and resulting in another ash-rich explosion. To date, however, the amount of ash from this episode has been small and confined primarily to the area around the caldera.

3. Characteristics of the Keanakāko‘i Drainage Networks

[15] A gully is defined as a drainage depression that transmits ephemeral flow, has steep sides, a steeply sloping or vertical head scarp, a width greater than 0.3 m, and a depth greater than 0.6 m [*Brice*, 1966]. Gullies commonly form in weak, unconsolidated materials such as loess [*Brice*, 1966], volcanic tephra [*Blong*, 1970], alluvium, colluvium, and gravels [*Stocking*, 1980]. They may be continuous or discontinuous, although combinations of the two are possible.

[16] Continuous gullies typically form in non-cohesive materials that do not have a resistant sediment cap or stabilizing vegetation coverage. They often begin as a small rill that increases in width and depth downslope as the contributing area increases. In the upper reaches, the slope of a continuous gully tends to be steeper than the slope of the surrounding terrain, and the gully maintains a V-shaped cross-sectional profile. In the medial reaches, gully slope decreases. Flows may remove material from the steeply sloping gully sides and a low-relief floor develops, generating a more rectangular cross profile. In the lower reaches, slope declines further, and increased deposition can lead to the formation of a fan that extends beyond the mouth of the gully [*Selby*, 1993].

[17] Discontinuous gullies commonly form where the resistant sediment capping has been disrupted (e.g., by surface runoff) or the stabilizing vegetation has been disturbed (e.g., by fire or livestock). Initially, a series of small isolated gullies form downslope of small knickpoints (headcuts) that are associated with small plunge pools. These discontinuous sections are typically deeper than they are wide, and the slopes are less than the surrounding terrain, so eroded material forms small fans upslope of the next knickpoints. Overtime the knickpoints advance upslope, and the previously discontinuous sections of gullies begin to coalesce. Eventually a single gully with a slope roughly equivalent to the surrounding terrain may develop [*Leopold et al.*, 1992].

[18] In the upper reaches of the Keanakāko‘i, gullies are either continuous or discontinuous depending on which tephra unit they have incised. Near the drainage divides, the gullies are confined to the upper, lithic unit of the Keanakāko‘i tephra and tend to be discontinuous. The fine-grained ash layers, some of which contain accretionary lapilli, are indurated and resistant to erosion, whereas the coarser-grained tephra layers are more easily eroded. This strength difference between the ash and coarser tephra layers generates a series of amphitheater-shaped knickpoints with

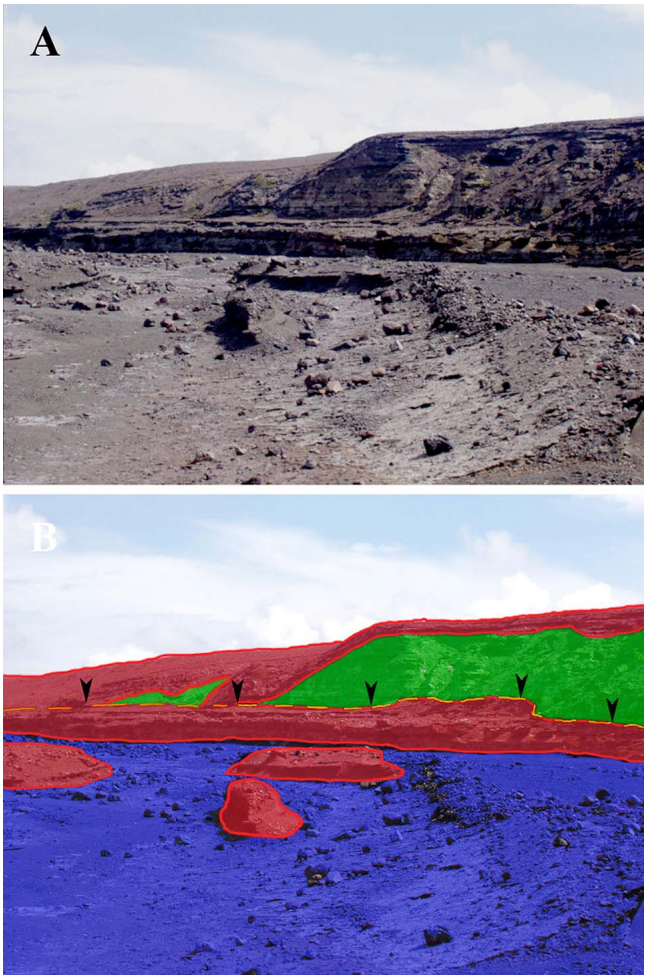

Figure 3. (a) The junction between Sand Wash (foreground) and a large tributary (background); when present, the flow direction is roughly toward the camera. During the 1980s the prevailing paradigm was that the Keanakāko‘i tephra had been emplaced entirely during the phreatic eruption that occurred in 1790 [*Malin et al.*, 1983; *Decker and Christiansen*, 1984]. However, the colored image on the bottom (b) shows that fluvial erosion had occurred within the lower, vitric unit of the Keanakāko‘i tephra (green) prior to the emplacement of the upper, lithic unit (red), implying a hiatus in the deposition of the tephra. The lithic deposits blanket the vitric deposits and fill a pre-existing gully. Subsequent erosion through most of the tephra has created a terrace along the margins of the valley (bench marked by arrows in Figure 3b) and left erosional remnants within Sand Wash that occur as small islands or large blocks on the surface (isolated red objects in the foreground of Figure 3b).

associated plunge pools (Figure 4a). Initially, the gullies form small depressions in the fine-grained ash layers, but once those layers have been breached, the gullies dramatically increase in both width and depth forming a plunge pool from which larger channels exit and continue downslope. Knickpoints and plunge pools get progressively larger as the contributing area increases downslope (Figure 4b). Likewise, many gullies and channels dramatically increase in width and depth downslope; beginning as depressions only a few centimeters deep and tens of centimeters of wide and ultimately becoming up to meters larger in both width and depth. Along these gullies and channels, basal undercutting of the more resistant ash layers during floods creates a series of cantilevers that overhang the banks. Failure of the cantilevers occurs after the water has disappeared, creating irregularly spaced scallops along the banks and leaving blocks of material on the gully and channel floors (Figure 5). Locally, these cantilevers can be long (>10 m), and failure can dramatically widen the gully or channel at specific locations. In plan view, it is apparent that the additional flow supplied by a tributary does not always increase the likelihood that cantilevers will develop, and in some locations, gully or channel widths actually decrease where tributaries join the main channels (Figure 6a). This is not generally true of drainage networks and may reflect control exerted by the resistant ash layers that occur in the Keanakāko‘i tephra.

[19] The gullies and channels that have eroded into the lower, vitric-rich part of the Keanakāko‘i tephra are continuous and tend to form a single, integrated feature that more closely parallels the slope of the surrounding topography. The lower unit of the Keanakāko‘i tephra is well sorted, which makes it slightly more cohesive than the upper lithic unit. Once flow begins to incise into the lower, vitric unit, cantilevers are not as common, the banks tend to be more vertical (as demonstrated in Figure 2), and the gully and channel floors also tend to be low-relief or virtually flat. Gully and channel incision into the lower part dramatically increases widths by almost a factor of two (Figure 6a), but width remain highly variable, probably owing to localized undercutting and collapse of the upper lithic-rich tephra unit.

4. Hydraulic Conductivities, Flow Velocities, Discharge, and Erosion Rates

[20] Many of the morphological characteristics of the Keanakāko‘i drainage networks described above are indicative of an ephemeral flow regime. In particular, the widespread presence of discontinuous gullies with knickpoints, irregular downstream width changes, and evidence of collapsed blocks with few signs of reworking on typically low-relief gully/channel floors (Figures 3, 4, and 5) all indicate a flow regime dominated by short-lived flood events that rise and recede rapidly, and then are followed by long periods of little or no flow. Descriptions of drainage networks that incise into tephra with perennial, stable flow [e.g., *Woolfe and Purdon*, 1996] have highlighted different morphological characteristics, including well-developed flights of cut and fill terraces, meanders with scroll and point bars, and bed forms, including ripples and dunes, all which are consistent with extended reworking and sorting of transported sediment.

[21] Owing to the remoteness of the Ka‘ū Desert and the unpredictability and rarity of runoff-generating precipitation events, little is known about flow hydraulics in the gullies and channels. The drainage networks are ungauged, and anecdotal accounts of flows are limited. To assess the hydraulic conductivity of the Keanakāko‘i tephra, we conducted a number of field experiments on both the upper and lower units. To estimate flood flow velocities and potential discharge, we used three different methods that are based on:

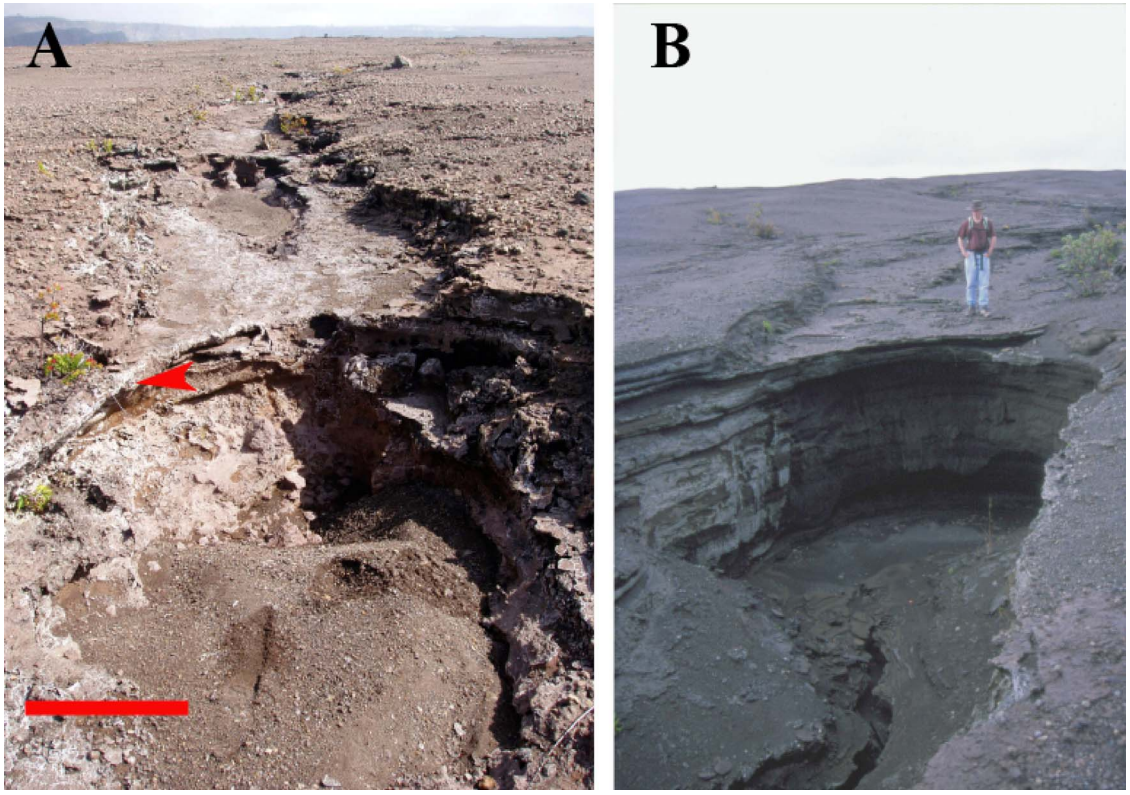

Figure 4. (a) Amphitheater-shaped gully headwalls and knickpoints with associated plunge pools (dry between ephemeral flow events) are common characteristics of the Keanakako'i drainage networks. They are controlled by the contrast in strength between the finer-grained ash layers (arrow), which are relatively resistant to erosion, and the interbedded coarser-grained tephra layers, which are more easily eroded. In this image the kickpoint close to the gully head contains a small pool only a few centimeters deep. The scale bar on the bottom left is approximately 5 cm wide. (b) Further downslope, knickpoints become larger, and the pools increase in size to tens of centimeters depth.

1) the physical parameters of the gullies and channels (the depth-slope method); and 2) the characteristics of the transported sediments (the sediment method and the friction factor method). Ideally, the different methods should produce similar results for flow velocities, thus providing a mechanism for checking and verifying the estimates, and generating greater confidence in subsequent discharge and erosion rate estimates.

4.1. Hydraulic Conductivity Estimates

[22] Hydraulic conductivity, k, is sometimes known as the coefficient of permeability and describes the ease that water can move through a material. If the Keanakāko'i tephra is considered a proxy for the Martian surface, then determining the hydraulic conductivity could be useful for constraining models of groundwater flow on Mars. Because hydraulic conductivity can also be related to the infiltration capacity of the soil [*Horton*, 1933], it is also an important parameter for assessing the environmental conditions necessary to generate surface runoff. There are a number of empirical and experimental approaches for determining hydraulic conductivity. In our study, we conducted field experiments on the tephra using a mini disk infiltrometer manufactured by Decagon Devices. This infiltrometer consists of a calibrated, clear plastic tube separated into two chambers both of which are filled with water. The upper chamber controls the suction, and the lower chamber contains the volume of water that is allowed to infiltrate into the tephra at a rate determined by the suction in the upper chamber. The bottom of the infiltrometer consists of a sintered, stainless steel disk that is porous and does not allow water to leak out of the chamber in the open air.

[23] The infiltrometer was placed on flat, clean exposures of both the upper and lower units of the Keanakāko'i tephra in different locations. As water began to infiltrate into the tephra, we recorded the volume (mL) at regular, 10-s intervals. The cumulative infiltration (cm) was calculated and plotted as a function of the square root of time. A regression analysis was performed graphically on the data and the slope of the line was determined, using a method proposed by *Zhang* [1997]

$$k = C_1/A \tag{1}$$

where k is the hydraulic conductivity of the soil (cm/s), C_1 is the slope of the line (cm/s) and A is a value relating the van Genuchten parameters for a given soil type to the suction

Figure 5. This is an example of a channel that has incised the upper, lithic unit of the Keanakāko‘i tephra. Flow is in the direction of the camera. The gully is ~4.5 m across. During ephemeral floods the fine ash layers remain relatively resistant, but erosion of the weaker tephra layers results in undercutting and corrosion. This erosion creates a series of cantilevers that overhang the banks, which eventually fail and fall into the channel. Large blocks of failed cantilevers can be seen sloping into the channel on both sides.

rate and radius of the infiltrometer disk. For sandy soil and suction of −2 cm (which was calibrated by the water level in the upper chamber), A = 1.73. For the upper unit of the Keanakāko‘i tephra we determined values of k ranging from 0.003 to 0.027 cm/s. Typically, lower values of k were associated with thick surface coatings of amorphous silica and jarosite, which are deposited as a result of the interaction between sulfur dioxide gases released by Kilauea and wicking of fluids contained in the pore spaces of the Keanakāko‘i tephra [*Schiffman et al.*, 2006]. For the lower unit of the Keanakāko‘i tephra we determined values of k ranging from 0.013 to 0.028 cm/s. Values of k were found to be ~0.023 cm/s for material deposited on the floor of one of the largest drainage channels, which is referred to as Sand Wash. The range of values for k that we measured on the Keanakāko‘i tephra are equivalent to 10 to 10^2 darcies, which are typical values of permeability expected for material composed of clean sand and loose, unconsolidated gravel [*Freeze and Cherry*, 1979, p. 29].

4.2. Flow Velocity: Depth-Slope Method

[24] The simplest method for estimating flow velocity within a gully or channel is the depth-slope formula where the bed shear stress of a flow, or the retarding stress at the base of a flow, t_b, is calculated by the equation

$$t_b = \rho g h S \tag{2}$$

In this equation ρ is the density of the fluid (998.2 kg/m^3, water at 20°C), g is gravitational acceleration (9.80 m/s^2), h is the flow depth (in meters and estimated from field observations in several places along the walls of the gullies and channels), and S is the bed slope of the gully or channel (measured directly from several different DGPS surveys of the gully/channel long profiles and confirmed from available topographic data; Figures 6b, 7). Flow depths were difficult to estimate, primarily because slumping and cantilever failure occur during and after flow events (Figure 5), obscuring the gully walls and channel banks. In addition, amorphous silica coatings resulting from outgassing from Kīlauea quickly form on most exposed surfaces of the Keanakāko‘i tephra, particularly near the caldera [*Schiffman et al.*, 2006]. This coating completely obscures many subtle textures, such as high water marks that may have eroded into the gully walls or channel banks. Where we did find suggestions of high water marks, it appeared that that flow within Sand

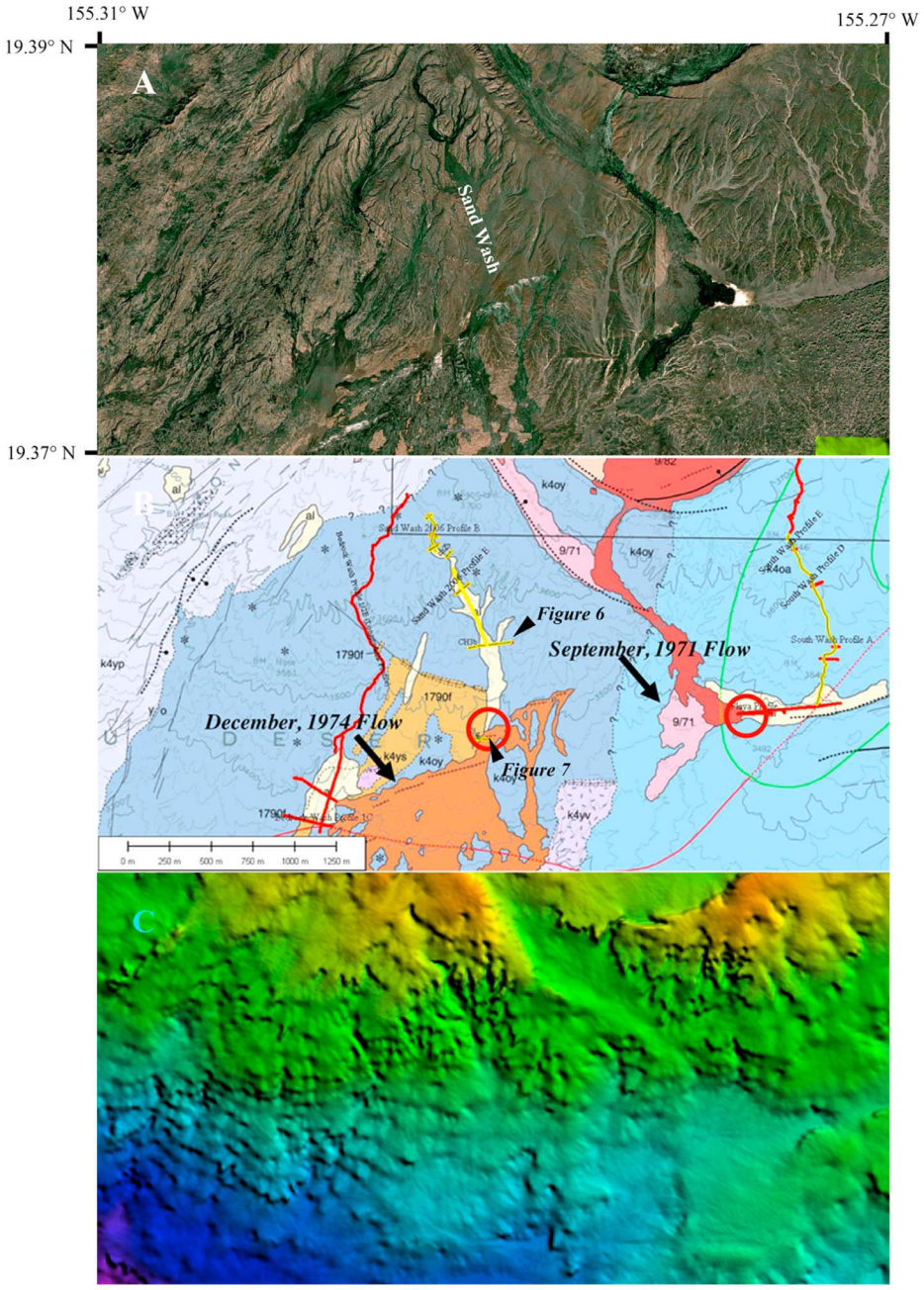

Figure 6. Different views of the Keanakāko‘i drainage networks. (a) GEX images of the drainage networks show their location with respect to the caldera. Sand Wash is labeled. The image is centered at 19.38°N, 155.29°W. (b) A geologic map of the area shown in Figure 6a [*Neal and Lockwood*, 2003]. Topographic survey lines are shown in red and yellow and represent data collected in two different years. Note the location of the December, 1974 and September, 1971 flows. Material eroded from the Keanakāko‘i tephra and transported as bed load during ephemeral flows overlies these lava flows, and trenches were dug in two locations showing the contact (red circles). Scale bar is 1250 m. (c) USGS 10-m topographic data used to estimate the volume of material eroded from Sand Wash. Orange represents high elevations (1153 m max) and blues and purple are lower elevations (950 m min).

Wash may have been ~0.10–0.50 m deep. Bed slope is also variable; in the headwaters of Sand Wash the slope was measured at 0.0308, but it rapidly increased to 0.0485 down channel. Both values for slope were used in our calculations.

[25] The bed shear stress can be equated to the bottom stress created by a flow, t where

$$t = \rho C_f \overline{u}^2 \quad (3)$$

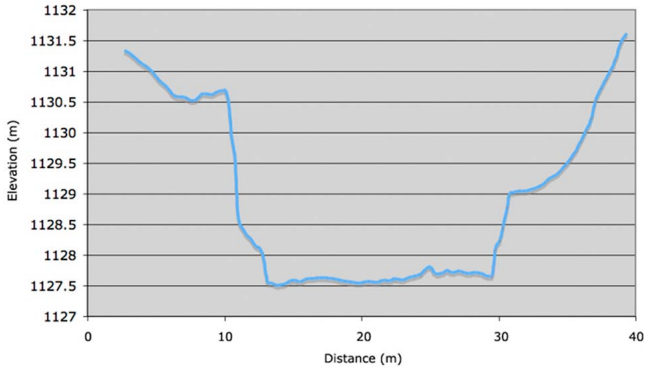

Figure 7. A representative cross-section of Sand Wash derived by the DGPS survey. The location of this profile is shown in Figure 6b. Note the low-relief of the floor, which is typical of the drainage networks that have incised into the lower vitric unit of the Keanakāko'i tephra.

Here C_f is a dimensionless drag coefficient, and $\bar{u}$ is the mean flow velocity (m/s). Thus, the mean flow velocity within a gully or channel can be calculated from

$$\bar{u} = \left(\frac{ghS}{C_f}\right)^{1/2} \quad (4)$$

The dimensionless drag coefficient can be adjusted for gravity by the expression

$$C_f = g\left(\frac{n^2}{h^{1/3}}\right) \quad (5)$$

where n is the Manning roughness coefficient (units of $s/m^{1/3}$), which has been derived empirically from terrestrial observations. Application of an appropriate Manning roughness coefficient, n, involves a certain degree of subjectivity, but values ranging from 0.015 to 0.035 are typically used to describe most relatively smooth, low sinuosity channels free of large-scale roughness elements (e.g., bedrock outcrop, boulders, vegetation [*Barnes*, 1967]), which characterizes many gully and channel reaches incised into the Keanakāko'i tephra. These values of Manning's n have also been applied to the Martian surface [e.g., *Komatsu and Baker*, 1997]. From equations (2)–(5), we estimated that the mean flow velocity within the gullies and channels was ~0.5 to 4.0 m/s (Table 1).

4.3. Flow Velocity: Sediment Method

[26] An alternative method for estimating flow velocities can be made directly by analyzing the particles sitting on the dry gully and channel beds. This involves a statistical analysis of the particle size and then determination of the hydrologic conditions necessary to transport the material. We collected a series of surface samples from the fluvial deposits within the Keanakāko'i drainage networks. Because there are typically cross-sectional variations in the sediment transport rates within a channel [*Leopold and Emmett*, 1997], we also conducted particle size analyses across the gullies and channels within 1-m^2 bins at regularly spaced intervals (roughly every 1–2 m depending on width) to determine a statistically representative particle size for the channel cross-section at a particular location. Samples were then dry sieved at 1-phi size intervals and weighed.

[27] *Shields* [1936] derived empirical relations to show how the critical shear stress required to initiate motion in a flow is a function of particle size. The nondimensionalization of the two parameters, the dimensionless grain parameter (ζ_*) and the dimensionless boundary shear stress (τ_*), allows comparison between the forces moving the particle (shear stress) and the forces causing the particle to remain in place (particle size and density). From an analysis of the particle size, we can determine the dimensionless grain parameter, which is defined as

$$\zeta_* = \frac{D^3(\rho_s - \rho)g}{\nu^2\rho} \quad (6)$$

where D is the characteristic particle diameter (cm), which was determined from our sieve analyses, ρ_s is the density of the particle (assumed to be basalt at 2.5 g/cm^3), ρ is the density of the fluid (i.e., water at 20°C), g is the acceleration of gravity (980 cm/s^2), and ν is the kinematic viscosity of the fluid (water at 20°C or 1.004×10^{-2} cm^2/s). Although *Shields* [1936] specified the bed material size by its bulk mean size D_m, which for well-sorted and unarmored particle-size distributions can be expected to be similar to the bed surface median particle size (D_{50}), as a general rule the D_{84} grain size (the diameter at one standard deviation above the mean) is used to describe the largest particle transported in saltation (as opposed to bed load) during flow. Typical measured values of the D_{84} grain size ranged from 0.174 to 0.325 cm (very coarse sand to very fine gravel). Note also that unlike the depth-slope method, parameters in the sediment method are expressed in cgs units.

[28] From *Shields*' [1936] curve, values for the dimensionless boundary shear stress (τ_*) can be determined. For

Table 1. Estimated Flow Velocities Within Sand Wash Using Equations (2)–(5)

Manning's n	Slope *(S)*	Flow Depth, h (m)	Average Flow Velocity, [a] (m/s)
0.015	0.0308	0.01	0.54
		0.10	2.52
		0.30	5.24
		0.50	7.37
0.025	0.0308	0.01	0.32
		0.10	1.51
		0.30	3.15
		0.50	4.42
0.035	0.0308	0.01	**0.23**
		0.10	1.08
		0.30	2.45
		0.50	3.16
0.015	0.0485	0.01	0.68
		0.10	3.16
		0.30	6.58
		0.50	**9.25**
0.025	0.0485	0.01	0.41
		0.10	1.89
		0.30	3.95
		0.50	5.55
0.035	0.0485	0.01	0.29
		0.10	1.36
		0.30	3.07
		0.50	3.96

[a]Maximum and minimum flow velocities are marked in bold for clarity.

Table 2. Estimated Flow Velocities Within Sand Wash Using Equations (6)–(11).

Manning's n	Grain Diameter, D_{84} (cm)	Sheer Velocity, u_* (m/s)	Flow Depth, h (m)	Average Flow Velocity, [a] (m/s)
0.015	0.174		0.01	0.32
0.015	0.2297		0.01	0.37
0.015	0.3248		0.01	0.44
0.025	0.174		0.01	0.19
0.025	0.2297		0.01	0.22
0.025	0.3248		0.01	0.27
0.035	0.174		0.01	**0.14**
0.035	0.2297		0.01	0.16
0.035	0.3248		0.01	0.19
0.015	0.174		0.10	0.48
0.015	0.2297		0.10	0.55
0.015	0.3248		0.10	0.66
0.025	0.174		0.10	0.29
0.025	0.2297		0.10	0.32
0.025	0.3248		0.10	0.39
0.035	0.174		0.10	0.20
0.035	0.2297		0.10	0.24
0.035	0.3248		0.10	0.28
0.015	0.174		0.30	0.57
0.015	0.2297		0.30	0.66
0.015	0.3248		0.30	0.79
0.025	0.174		0.30	0.34
0.025	0.2297		0.30	0.40
0.025	0.3248		0.30	0.47
0.035	0.174		0.30	0.25
0.035	0.2297		0.30	0.28
0.035	0.3248		0.30	0.34
0.015	0.174		0.50	0.62
0.015	0.2297		0.50	0.71
0.015	0.3248		0.50	**0.85**
0.025	0.174		0.50	0.37
0.025	0.2297		0.50	0.43
0.025	0.3248		0.50	0.51
0.035	0.174		0.50	0.27
0.035	0.2297		0.50	0.31
0.035	0.3248		0.50	0.37

[a]Maximum and minimum flow velocities are marked in bold for clarity.

values of ζ_* less than ~400, *Shields* [1936] extrapolated his curve, but empirical data can be used to determine values for τ_* in this range [*White*, 1970]. For values where $\zeta_* > 10{,}000$, τ_* approaches a constant of 0.045. *Brownlie* [1981] describes a useful fit to Shields' data as

$$\tau_* = 0.22\zeta_*^{-0.6} + 0.06\exp\left(-17.77\zeta_*^{-0.6}\right) \quad (7)$$

The dimensionless boundary shear stress, τ_* is

$$\tau_* = \frac{\tau_{cr}}{(\rho_s - \rho)gD} \quad (8)$$

where τ_{cr} is the critical boundary shear stress needed to initiate sediment motion. In most instances τ_{cr} is also assumed to be the bottom shear stress, τ_b, during flooding. Basically, we assume that the flow through the gully or channel is at least fast enough at the bed to initiate sediment transport of the D_{84} particle. The threshold shear velocity, u_* (expressed in cm/s), is

$$u_* = \sqrt{\frac{\tau_{cr}}{\rho}} = \sqrt{\frac{\tau_b}{\rho}} \quad (9)$$

By substituting equation (2) for τ_b, equation (9) becomes

$$u_* = \sqrt{ghS} \quad (10)$$

Since the other parameters are known (g and S), this approach also allows us to solve for h, the depth of flow through the channel, providing us with an independent way of checking our field observations. Application of equation (10) suggests that flow through Sand Wash only need to be on the order of a centimeter or two deep in order to initiate movement of the sediment (Table 2). This would appear to be due primarily to the steep slopes through Sand Wash.

[29] As *Komar* [1979, 1980] notes, it is better to analyze the flow in terms of u_* than $\bar{u}$ due to the uncertainties in estimating reasonable values for C_f. However, values of $\bar{u}$ are more intuitive. These can be calculated from the relationship

$$\overline{u} = \left(\frac{1}{C_f^{1/2}}\right)u_* = \left(\frac{h^{1/6}}{g^{1/2}n}\right)u_* \quad (11)$$

To estimate values of $\bar{u}$ through this method, again we adopt Manning coefficient values of 0.015 to 0.035 to reflect that many gullies and channels reaches lack large-scale roughness elements. It is also important to note that values of u_* must be converted to MKS units (m/s) to be applicable to equation (11). Results from this method suggest that flow velocities ranged from ~0.2 to ~0.8 m/s (Table 2).

4.4. Flow Velocity: Friction Factor Method

[30] As described above, paleoflow depth and velocity can be estimated from the critical shear stress, τ_{cr} (N/m^2), needed to initiate sediment movement. *Shields* [1936] criterion represents τ_{cr}, which can be used to determine a minimum or threshold flow depth H_t (m) by

$$H_t = \tau_{cr}/\gamma S \quad (12)$$

where S (m/m) is the slope (0.0308 near the headwaters and 0.0485 down channel), and γ (N/m^3) is the specific weight of water (i.e., density, ρ (kg/m^3) times gravitational acceleration, g (m/s^2)). Critical shear stress, τ_{cr}, is calculated using the semi-empirical function

$$\tau_{cr} = \tau_*(\gamma_s - \gamma)D \quad (13)$$

where τ_* is the Shields coefficient (dimensionless boundary shear stress), γ_s is the specific weight of sediment (N/m^3), and D (m) is the grain size, where D is larger than ~0.2 mm. For reference, typical density values are ρ_s = 2800 kg m^{-3} for basalt and ρ = 1000 kg m^{-3} for clear water. The coefficient τ_* is assumed here to have Shields' original value of 0.045; however, this value may vary from as low as 0.01 to as much as 0.1 depending on sediment sorting, particle shape, and particularly on the looseness of packing of the boundary [*Church*, 1978], with typical values ranging from 0.03 to 0.06 [*Komar*, 1988].

[31] Under the assumption of steady, uniform (i.e., constant depth) flow in a channel that has a rigid boundary (i.e., flow conditions up to bed motion), the threshold mean flow

velocity for sediment transport, v_t (m/s), can be computed based on resistance coefficients and channel geometry by two widely used methods. The first employs the Manning roughness coefficient, n:

$$v_t = \left(R^{0.67} S^{0.5}\right)/n \quad (14)$$

and the second uses the Darcy-Weisbach friction factor, f:

$$v_t = \left[(8\, g\, R\, S)/f\right]^{0.5} \quad (15)$$

where R (m) is the hydraulic radius (ratio of flow cross-sectional area to wetted perimeter, which is comparable to flow depth H in channels with a high width/depth ratio $>\sim$15). Unlike the empirical Manning-type equation, the Darcy-Weisbach equation uses a dimensionless friction factor, has a sound theoretical basis, and explicitly accounts for the acceleration from gravity; moreover, the relative roughness does not influence the exponents of hydraulic radius [*Raudkivi*, 1967] and slope [*Liu and Hwang*, 1959]. For these reasons, the Darcy-Weisbach equation is often preferred over the Manning approach [*Silberman et al.*, 1963; *Kleinhans*, 2005]. Overestimating or underestimating the flow depth not only affects the discharge but also the velocity through the roughness equation (equations (14) and (15)).

[32] We use empirically derived relationships to estimate the resistance coefficients (n and f). *Limerinos* [1970] related the roughness coefficient to flow depth and D_{84}:

$$n = \left(0.113 R^{0.167}\right)/(1.16 + 2.0\, \log(R/D_{84})) \quad (16)$$

based on data from primarily lower-gradient channels with bed material composed of small gravel to medium-sized boulders. *Bray* [1979] used a data set of gravel bed rivers with similar gradients and revised equation (16) as:

$$n = \left(0.113 R^{0.167}\right)/(1.09 + 2.2\, \log(R/D_{84})) \quad (17)$$

For the Darcy-Weisbach friction factor, *Hey* [1979] developed an equation based on twenty-one straight, gravel bed rivers in the United Kingdom and determined that the roughness height, k_s, is best approximated by $3.5D_{84}$ in coarse-grained (gravel and cobble) natural channels with width/depth ratios >15 and $R/D_{84} > 4$:

$$\left(1/f^{0.5}\right) = 2.03\, \log(a\, R/3.5D_{84}) \quad (18)$$

The value for a may be determined graphically [*Hey*, 1979] or, as suggested by *Thome and Zevenbergen* [1985], from the relationship

$$a = 11.1\, (R/H_{max})^{-0.314} \quad (19)$$

Using this approach, we estimate that the flow depths were <0.01 m and flow velocities of $\sim$0.22 m/s were necessary to mobilize the fine gravel particles in Sand Wash.

4.5. Estimated Discharges and Erosion Rates

[33] The estimated average flow velocities in Sand Wash calculated from the first method (equations (2)–(5); Table 1) varied considerably from $\sim$5.0 to 200 cm/s (i.e., 0.05–2.0 m/s). In part this range reflects our inability to accurately determine the flow depth in the field, but it also suggests that the drainage network morphology has the potential for higher velocity flows. Using the second method (equations (6)–(11)) the estimated flow velocities (Table 2) were more consistent at $\sim$1–8 cm/s (i.e., 0.01–0.08 m/s). The third method (equations (12)–(19)) provided flow depths similar to those determined by the other two methods and flow velocities that were higher ($\sim$0.22 m/s), but still broadly consistent with at least the first method. Ideally, the three approaches should provide flow estimates that are similar, but in our analyses only the lower flow velocities (<0.10 m/s) are consistent. This implies that when the channels are active typical flow depths are on the order of 0.01–0.10 m with average velocities of $\sim$0.10 m/s. Sand Wash is a maximum of $\sim$20 m wide (Figure 7), so assuming a flow depth of 0.10 cm, this would result in discharges of $\sim$0.2 m^3/s in Sand Wash at its widest point.

[34] How long would it take to erode the gullies and channels throughflows with these typical discharges? Similar exercises have been performed for both Martian outflow channels [*Komar*, 1980; *Carr*, 1996, p. 62] and Martian valley networks [e.g., *Irwin et al.*, 2005b], and several approaches can be taken to make this estimate. Perhaps the most straightforward approach involves estimating the total volume of sediment removed from Sand Wash and comparing that to the age of the Keanakāko‘i tephra. From available digital elevation models of Kīlauea (Figure 6c), we estimated the total volume of removed sediment from Sand Wash and its tributaries to be roughly $\sim 2.5 \times 10^4$ m^3, removed from an area of 625,000 m^2, for an average denudation of 0.04 m. From the ^{14}C ages collected from the base of the Keanakāko‘i tephra [*Swanson et al.*, 2004, 2012] incision of the drainage networks probably began about 1500 AD. Consequently, material has been eroded at an average rate of $\sim$50 m^3/yr, or 8×10^{-5} m/yr averaged over the area. For comparison, total precipitation over this time would be about 650 m at 1.3 m/y, about 16,000 times the eroded depth. If sediment concentrations are $\sim$40% by volume of the total discharge [e.g., *Komar*, 1980], then sediment transport through Sand Wash would last for an annual average of $\sim$600 s, or $\sim$10 min. As we discuss below, however, the storms necessary to initiate runoff do not occur every year but are highly episodic. When they do occur flows would nonetheless tend to be short-lived, probably owing to widespread transmission losses in the normally dry, highly permeable channel bed sediments, which is supported by the hydraulic conductivity measurements that we made. Although quantitative data are lacking, it is possible that most competent flows last for less than an hour.

5. Climatic Conditions

[35] The field observations and calculations presented above indicate that flows in the Keanakāko‘i drainage networks are ephemeral and short-lived. Despite the annual rainfall of $\sim$130 cm, the inference is that only high magnitude rainfall events are capable of generating surface runoff and widespread flow events in the drainage networks. Additional information supports this inference. As an example, on September 1, 2003, Hurricane Jimena passed within 165 km south of the Big Island. The area received approximately 15 cm (6 in) of rain within a few hours, but we only observed small puddles on the surface of the

Figure 8. A trench dug into sediments (see Figure 6b for location) overlying the December 1974 flow (indicated by the orange arrow) provides evidence that there has been ~10 later storm events in the Ka‘ū Desert capable of generating runoff and flow through the drainage networks developed in the Keanakāko‘i tephra. Each flow event is represented by a flood couplet ~5 cm thick that comprises a coarser- and finer-grained layer. An analysis of state climatic records indicates that the storms with the highest precipitation typically occur during the winter months when southerly winds create prolonged stationary disturbances, generating so-called “kona storms.”

Keanakāko‘i tephra. One of the last reported flows within the Keanakāko‘i drainage networks occurred in November 2–3, 2000, when the area received almost 75 cm (30 in) of rain within a 24-h period. From March 9 to 11, 2006, the Hawaiian Volcano Observatory measured almost 28 cm (11 in) of rain, which was enough to initiate surface runoff and some flow through the bedrock channels that intersect Hilina Pali Road farther downslope.

[36] To provide more information relating to the climatic conditions necessary to generate flows within the drainage networks, we identified two locations where sediment from the flows was deposited on top of lava flows of known ages, including a flow that erupted from fissures near Halema‘uma‘u in September 1971 and another flow that erupted from fissures in the southwest rift zone in December 1974 (Figure 6b). Trenches excavated into the fluvial deposits showed that at each location there were ten sediment couplets, each consisting of a very coarse (gravelly sand) and a finer-grained (sand) layer (Figure 8). Each couplet is interpreted as a deposit from a single flow event, representing sediment deposited during peak and waning flow stages, respectively. Together these couplets suggest that there have been ten climatic events since September 1971 that were capable of generating widespread flow within the Keanakāko‘i drainage networks. Available climatic records from weather stations within the Ka‘ū District were searched, with Table 3 listing the dates for the ten most significant rainfall events since 1971. These events included 21–43 cm of rain locally over a 24-h period, with additional rainfall in the day before or after. Taken together, these ten storms produced 3.02 m of rain on their peak days. Taking this value as the total effective rainfall over 40 years, then the denudation of ~0.04 m was accomplished with ~40 m of rainfall over ~500 years. Even when rainfall that did not produce runoff is neglected, and we look only at the most intense storms, the available precipitation was on the order of a thousand times the eroded depth.

[37] Typically the prevailing winds are northeasterly trade winds, and because of the orographic effects generated by Kīlauea most of the precipitation occurs on the northeastern slope of the volcano. In fact, during the summer months Volcano Village receives some rain almost every night, yet only a few miles west across the summit, the leeward the Ka‘ū Desert commonly stays dry. Analyses of the climate data for the state of Hawaii indicate that the weather systems generating the heaviest precipitation in the Ka‘ū Desert are due primarily to stationary disturbances with strong southerly winds that are near-surface. During these conditions, the southeastern part of Hawaii becomes windward, and precipitation is topographically enhanced in the elevated terrain. With the abundance of moisture from the lower latitudes, if the atmosphere is unstable, the conditions are set for heavy rainfall that can occur over a 48–72 h period. As Table 3 shows, such conditions usually occur during the winter months, and 9 out of 10 of the largest storms in the last 40 years are associated with major storms known locally as kona storms. A kona storm is typically a nonfrontal low-pressure system that can last for days or weeks without weakening and can bring flooding to the islands [e.g.,

Table 3. The Ten Most Significant Rainfall Events in the Ka‘ū Desert Since 1971.

			Station Precipitation (in)		
Year	Month	Day	Hawaii NP	Pahala	Pahala Mauka
1979	2	20	16.75	16.96	
		21	5.85	1.91	
1980	3	17	6.02	4.67	
		18	10.72	25	
1981	12	25	4.97	4.65	
		26	12.95	11.9	
1987	12	13	12.96		8.85
		14	3.2		3.19
1990	1	19	2.48		1.86
		20	10.64		12.95
1990	11	20	9.72		5.7
		21	11.26		9.65
1994	9	19	12.26		6.52
		20	4.74		5.31
1996	3	3	8.43		9.1
		4	4.08		2.69
2000	11	2	missing		16.6
		3	missing		11.43
2001	11	27	10.52		8.35
		28	11.65		12.23

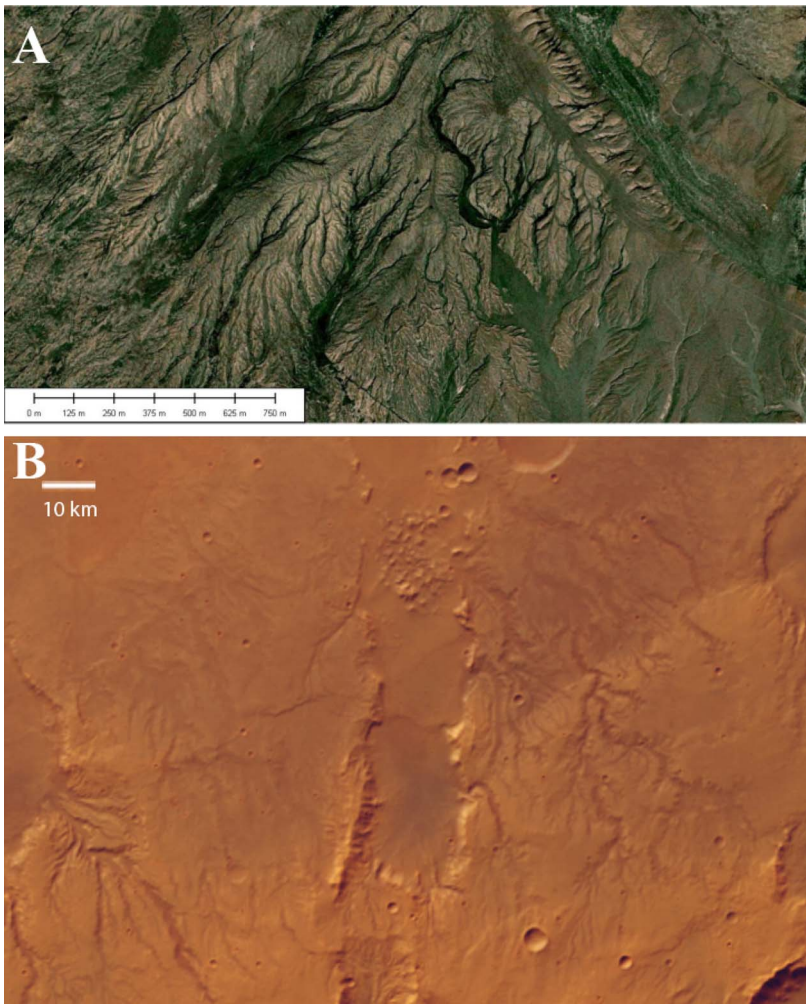

Figure 9. (a) In plan view, the widths of the Keanakakoʻi drainage segments vary considerably down-valley (enlargement from Figure 6a). While there is an overall downstream width increase, in some instances width actually decreases (e.g., at the junction with a tributary). Width variations occur independently of slope and are related to the variable resistance of the tephra layers. (b) Martian valley networks often display similar down-valley variations in width. Although such valley networks are often referred to as "degraded," suggesting that they have been modified since their formation, it is possible that local lithology exerted a strong influence. In this example, the valley networks have incised ejecta associated with the Huygens impact basin, which is likely brecciated and friable similar to the Keanakakoʻi tephra. (Photo ESA/DLR/FU Berlin, G. Neukum, SEM4NRMKPZD.)

Ramage, 1962; *Chu et al.*, 1993]. This quasi-stationary system appears on satellite images as large, comma-like cloud bands or masses with deep convection and rain to the east of the storm center.

6. Implications for Mars

6.1. Valley Networks

[38] The drainage networks that incise the Keanakākoʻi tephra are a couple of orders of magnitude smaller than most of the Martian valley networks, but they share three main morphologic characteristics. However, there are also some differences in morphology and inferred processes of development between the Keanakākoʻi and Martian drainage networks.

[39] First, many Keanakākoʻi gullies contain amphitheater-shaped headwalls (Figure 5), which is a common characteristic of many Martian valley networks (Figure 9). Unlike Martian networks, however, many Keanakākoʻi gullies contain a number of these amphitheater-shaped features at intervals along their course, many forming knickpoints and associated plunge pools that enlarge downslope as the contributing area increases. Furthermore, formation of amphitheater-shaped knickpoints is related to the difference in erodibility between the ash and coarser-grained tephra layers in the upper lithic unit of the Keanakākoʻi tephra under conditions of surface runoff, and is not a process related to groundwater sapping as has been suggested for Martian valley networks [e.g., *Pieri*, 1980]. In fact, the water table is over 500 m deep near the summit of Kīlauea [*Stearns and MacDonald*, 1946; *Zablocki et al.*, 1974], and there is no base flow in the streams, so the entire Keanakākoʻi drainage network has developed over recent centuries solely in

response to surface runoff and fluvial erosion. It is possible that the amphitheater-shaped heads of many Martian valley networks can be at least partly attributed to similar differences in lithology [*Craddock and Howard*, 2002; *Lamb et al.*, 2006; *Irwin et al.*, 2009], irrespective of whether surface runoff or groundwater is the main erosive agent. Potentially, the upper crust of Mars may be capped by more resistant strata, such as indurated sediments [*Binder et al.*, 1977; *Howard et al.*, 2005] or a layer of volcanic material [*Malin and Edgett*, 2001], which is then underlain by more erodible, brecciated or friable material.

[40] Second, although the average widths of the Keanakāko'i drainage networks increase downslope, there is a great deal of local variability (Figures 6a and 9a). *Baker and Partridge* [1986] were the first to suggest that there are two classes of valley networks on Mars. Pristine valleys have steep sided walls, whereas degraded valleys have "eroded walls" that often result in valleys with irregular widths. Despite the fact that both pristine and degraded valleys occur in the same Martian drainage systems with pristine valley networks commonly occurring downslope, they suggested that the difference in morphology implied different ages and that the "degraded valleys" were older. More recently, *Hoke and Hynek* [2009] made similar interpretations of the age relationships of valley networks with comparable morphologies. While it is possible that the morphologic differences are due to age and preservation, *Hoke and Hynek* [2009] note that the difference in ages between the youngest and oldest valley networks they studied is only $\sim 210 \pm 50$ My. Given that it has been nearly 3.0 Gy since valley network formation processes ceased, it seems unlikely that such a small difference in age could produce such a dramatic difference in morphology. Instead, similar to the Keanakāko'i drainage networks, where width variations can be related to lithologically controlled differences in bank strength (Figure 5), the observed morphologic differences may be due to variations in local lithology. Martian valley networks that have incised into the rim of the Huygens impact basin, for example, exhibit many of the same morphologic characteristics observed in the Keanakāko'i drainage networks, including highly variable widths and valley widths that sometimes decrease at the junction with a tributary (Figure 9). It is probable that many Martian valley networks have incised into brecciated impact ejecta that is loose and friable not unlike most of the Keanakāko'i tephra. This concept suggests that it may be possible to use valley network morphology as a way of characterizing the general surface lithology on Mars.

[41] Third, many of the gullies and channels in the Keanakāko'i drainage networks have flat, low-relief floors and rectangular cross-sections (Figure 7), similar to many Martian valley networks. A number of investigators have interpreted the low-relief floors of Martian valley networks as indicative of formation by groundwater sapping [*Pieri*, 1980; *Goldspiel et al.*, 1993; *Gulick*, 2001]. Essentially, a rectangular valley cross-section would be expected to result from erosion along the contact between the perched aquifer and the underlying aquiclude. Given that the Keanakāko'i drainage networks have formed under conditions of surface runoff, however, cross-section morphology is most likely another adjustment to the characteristic ephemeral, short-lived sediment-transporting flows that transport abundant bed load in gullies and channels with variable bank strength. In similar transport-limited conditions, such as central Australia or southern and eastern Africa, channels commonly adopt a rectangular cross-section with a high width/depth ratio as this is thought to enable greater bed load transport either by directing a greater proportion of shear stress at the bed [*Mabbutt*, 1977] or by maintaining relatively high values of particle exposure (water depth: particle diameter) throughout flood events [*Reid and Frostick*, 2011].

[42] Finally, as described above, the amount of precipitation that has fallen in this area is on the order of 10^4 times the eroded depth, and when we consider only the peak rainfall days during the most intense storms, the rainfall is 10^3 times the eroded depth. The Keanakāko'i tephra is a relatively erodible material, so erosion of valley networks and degraded craters on Mars would have required large amounts of precipitation and runoff over time.

[43] These interpretations may have implications for reconstructing sediment transport conditions in Martian valley networks. It is unlikely that many Martian valley networks became fully graded before fluvial processes ceased as the longitudinal profiles of many valley networks are convex in shape and contain a number of knickpoints [*Aharonson et al.*, 2002; *Irwin and Howard*, 2002; *Kereszturi*, 2005; *Irwin et al.*, 2005b; *Ansan and Mangold*, 2006]. It is likely, however, that abundant sand and gravel particles were available for transport owing to ubiquitous impact brecciation, widespread volcanic eruptions [e.g., *Wilson and Head*, 2004], and possibly weathering effects. Because of the lower gravity on Mars, valley networks would have been more efficient at transporting sand-sized particles, and this can be described mathematically. For example, *Yalin* [1977] presents a detailed erosion equation that is expressed as

$$q_s = Kg^{1/2}D^{3/2}(S_s - 1)^{1/2}\left(\frac{Q^{3/5}n^{3/5}S^{7/10}}{W^{3/5}g^{3/10}(S_s - 1)D} - \tau'_{cr}\right)^P \quad (20)$$

where q_s is the rate of bed load transport, K is the erosional efficient factor (treated as a constant) [*Howard et al.*, 1994], g is gravity, D is the sediment grain size, S_s is the specific gravity of the sediment, S is channel slope, Q is the sediment transport capacity, n is the Manning coefficient, and W is channel width. Units are not provided here because this equation can be greatly simplified if the fluvial features on two planets are assumed to be identical. That is to say, if it were hypothetically possible to place the Keanakāko'i drainage network on Mars without changing any physical characteristics, then most of the terms cancel out and equation (20) becomes

$$q_s \propto g^{1/2}\left(\frac{1}{g^{3/10}}\right)^P \quad (21)$$

Basically, if all the physical variables are assumed to be the same, then bed load transport becomes proportional to gravity. There are empirically derived values of P, which is a function of grain-size. For sand-sized material P is 3.0 [*Einstein*, 1950], and for fine gravel P is 1.5 [*Meyer-Peter and Müller*, 1948]. As gravity is lower on Mars, and specific gravity is less, then in theory, transport of sand-sized particles is $\sim$50% more efficient. However, the exponent P

decreases with increasing grain sizes, reflecting the fact that lower gravity would also affect the weight of the water, which lowers the shear stress it would exert. Factoring this in, features identical to the Keanakāko'i drainage networks would be ~5% less efficient at transporting gravel-sized particles on Mars. Essentially, the Keanakāko'i-type drainage networks could remove the same amount of material in about half the time on Mars, but they would require slightly longer times to remove larger particles, and potentially they would take longer to incise into coarse material or bedrock. The combination of greater sediment loads and lower shear stresses implies that a channel would also adopt a rectangular cross section on Mars, but typically a Martian channel would be shallower and wider than a terrestrial channel.

6.2. Ancient Climate on Mars

[44] Although some climate models suggest that it may have been possible to create warm and wet conditions on early Mars [e.g., *Forget and Pierrehumbert*, 1997], numerous models suggesting the opposite also exist [e.g., *Colaprete and Toon*, 2003]. The major difficulty in resolving the early Martian climate comes from what *Sagan and Mullen* [1972] refer to as the "faint young Sun paradox." The Standard Solar Model suggests that stars similar to the Sun should brighten gradually over time [*Gough*, 1981]. This trend implies that at ~4.0 Gya the luminosity of the Sun was only about 70% of what it is today, which would make it difficult for liquid water to exist on the surface of both the Earth and Mars. Nevertheless, there is evidence for fluvial erosion on both Earth [*Sagan and Mullen*, 1972] and Mars [e.g., *Craddock and Howard*, 2002] during this time.

[45] If the early Martian surface consisted of brecciated basaltic material free of vegetation, by analogy with the Keanakāko'i drainage networks, runoff production and erosion of valley networks may have required heavy, intense rainfall at times. The ten most intense storms that have occurred in the Ka'ū Desert since 1971 all involved 21–43 cm (8–17 in) of rainfall averaged over a 24-h period (Table 3). Correlation with the fluvial strata deposited since that time suggest that such prolonged, intense precipitation is necessary to exceed the surface infiltration capacity, generate runoff, and transport sediments. Although terrestrial thunderstorms can produce rainfall with similar intensity, they are often short-lived, transient events that are not sustained in a single location for longer than about 30 min. Mesoscale convective storms are larger systems that cover a broader area, but they typically last for only a few hours. Larger, longer-lived storms include hurricanes, but based on the climate record in Hawaii they do not appear to have generated sufficient precipitation to initiate surface runoff, floods, and erosion in the Keanakāko'i tephra. This relative ineffectiveness may be because they move too fast and, as a result, are short-lived at the local scale. Early Mars may have experienced some other type of cyclonic storm system that was slower moving, similar to 'kona storms'. In fact, there are some recent climate models by *Richardson and Soto* [2008] and *Soto et al.* [2010] that demonstrate the feasibility of producing seasonal monsoons, similar to kona storms, on early Mars.

[46] *Richardson and Soto* [2008] and *Soto et al.* [2010] provide some of the first attempts at determining the global abundance and distribution of liquid water on the Martian surface. They ignored the faint young Sun paradox and assumed that, based on interpretations of the geologic evidence, the global mean surface temperature on early Mars was above freezing. Then they substituted terrestrial topography with Martian topography in the Community Atmosphere Model (CAM), which was designed by the National Center for Atmospheric Research (NCAR) and includes a hydrological model for coupling the interactions between water reservoirs contained in the oceans, land, and atmosphere [*Collins et al.*, 2004]. *Soto et al.* [2010] investigated four possible scenarios for the initial distribution of water: (1) an early Mars with no oceans but with a saturated regolith; (2) an early Mars with a northern ocean filled to −4.5 km elevation; (3) an early Mars with a northern ocean filled to −3.0 km elevation; and (4) an early Mars containing a distribution of highland lakes fed by valley networks [*Fassett and Head*, 2008b]. Under certain conditions (Scenario 3 with a large northern ocean in particular), heating of the southern highlands during southern summer could generate monsoon rains in the region where valley networks are concentrated. Meanwhile, low-pressure extratropical cyclones form and rain primarily over the northern ocean. Coupled with the field investigations presented here and the *Richardson and Soto* [2008] and *Soto et al.* [2010] models, it is possible that early Mars also experienced large, slow moving cyclonic storm systems capable of producing heavy rainfall amounts (tens of centimeters) over an extended period of time (days).

[47] Our analyses of the Keanakāko'i drainage networks may provide some additional information relevant to our understanding of the evolution of the Martian climate. Although stream incision to form the Martian valley networks appears to have been concentrated around the late Noachian/early Hesperian transition [*Howard et al.*, 2005; *Irwin et al.*, 2005b], fluvially modified impact craters suggest that fluvial processes in fact occurred throughout the Noachian, although with less tendency to downcut and remain preserved. Impact craters at all diameters are preserved in various states of degradation, and stratigraphically younger craters are less degraded than older ones of the same diameter, implying that modification occurred as impact craters were forming [*Craddock and Maxwell*, 1993; *Craddock et al.*, 1997; *Craddock and Howard*, 2002]. The ubiquitous occurrence of degraded craters suggests that climatic conditions capable of generating relatively intense precipitation were global in extent. This implies that perhaps crater modification was driven by the slow collapse of the primordial atmosphere, which also included some slow precipitation, but was primarily arid [*Craddock and Howard*, 2002]. Once water began to collect in the northern plains to form an ocean [*Parker et al.*, 1989; *Head et al.*, 1999], however, the climate became more complex and became organized in such a way as to be able to support local weather systems, including storms.

7. Conclusions

[48] The morphologic characteristics of the Keanakāko'i drainage networks are controlled by a combination of lithology and ephemeral flood flows generated by surface runoff. Although they are not good scale analogs to the Martian valley networks, they may represent good process analogs. In particular, their physical characteristics suggest

that several morphological features of Martian valley networks may be attributed to local lithology.

[49] First, the amphitheater-shaped gully headwalls and knickpoints in many Keanakāko'i drainage networks are controlled by the layers in the tephra, which vary in resistance. The ash layers provide a resistant capping, but once breached, the underlying, lithic-rich tephra is more easily eroded. Although the Martian regolith is friable, locally it may be capped by more erosion-resistant material, such as a thick, indurated duricrust or lava flow, which might also control the amphitheater-shaped morphology of the headwalls of Martian valley networks.

[50] Second, the highly variable width of the Keanakāko'i drainage networks is also a result of the different resistance of layers in the Keanakāko'i tephra. Lithic-rich layers forming the banks are easily eroded during ephemeral flooding, commonly resulting in basal undercutting and cantilever failure, and thus forming irregular gully or channel margins. Martian valley networks that exhibit similar morphologic characteristics most likely occur in materials that are also friable to some depth, such as crater or basin ejecta. In general, variations in valley network width may be a good proxy for the resistance of Martian surface material and may ultimately help us to understand the distribution of impact ejecta and Noachian-age lava flows.

[51] Third, the low-relief floors of the Keanakāko'i gullies and channels reflect the high proportion of sediment transported as bed load in high-energy but short-lived flood events. On Mars, the lower gravity means that sand-sized material would be more easily transported during floods; so flat-floored channels also may have been common.

[52] Because Martian valley network systems are poorly integrated with the surrounding cratered landscape, it is likely that valley network formation was short-lived and confined to around the late Noachian/early Hesperian transition [*Irwin et al.*, 2005b]. Our analyses of the Keanakāko'i drainage networks show that surface runoff and sediment transport occur only during major rainfall events when precipitation exceeds >2.5 cm (>1 in) an hour over a 24–48 h period. Moreover, erosion of this relatively friable material required storm precipitation on the order of 10^3 times the depth of denudation, suggesting that valley erosion on Mars required large amounts of precipitation over time. Climate modeling results suggest the possibility that the late Noachian/early Hesperian climate was also capable of supporting large cyclonic storms in the northern hemisphere and a summer monsoon in the south, if the northern lowlands contained an ocean [*Richardson and Soto*, 2008; *Soto et al.*, 2010]. Combined with our knowledge of the timing of crater modification on Mars [*Craddock and Howard*, 2002; *Mangold et al.*, 2012], the early climate of Mars appears to have had at least two phases: an initial arid climate that produced rainfall and limited surface runoff that may have been produced by the collapse of the primordial atmosphere, and a later, wetter climate that supported local weather systems, including major storms that may have been driven by the formation and persistence of a northern ocean.

[53] **Acknowledgments.** This research is supported by a grant from the NASA Mars Fundamental Research Program (NNX08AN64G). An award from the Smithsonian Institution's George F. Becker Endowment Fund supported preliminary fieldwork. The authors thank Corey Fortezzo, Brent Garry, Ruslan Kuzmin, Cathy Quantin-Nataf, Sharon Wilson Purdy, Don Swanson, and Jim Zimbelman for their support in the field. Don Swanson provided many useful comments on earlier versions of this manuscript. We also appreciate the constructive reviews received from Dave Crown and Nicolas Warner.

References

Aharonson, O., M. T. Zuber, D. H. Rothman, N. Schorghofer, and K. X. Whipple (2002), Drainage basins and channel incision on Mars, *Proc. Natl. Acad. Sci. U. S. A.*, *99*, 1780–1783, doi:10.1073/pnas.261704198.

Ansan, V., and N. Mangold (2006), New observations of Warrego Valles, Mars: Evidence for precipitation and surface runoff, *Planet. Space Sci.*, *54*, 219–242, doi:10.1016/j.pss.2005.12.009.

Baker, V. R., and J. B. Partridge (1986), Small Martian valleys: Pristine and degraded morphology, *J. Geophys. Res.*, *91*, 3561–3572, doi:10.1029/JB091iB03p03561.

Bandfield, J. L., V. E. Hamilton, and P. R. Christensen (2000), A global view of Martian surface compositions from MGS-TES, *Science*, *287*, 1626–1630, doi:10.1126/science.287.5458.1626.

Barnes, H. H., Jr. (1967), *Roughness Characteristics of Natural Channels*, *U.S. Geol. Surv. Water Supply Pap.*, *1849*, 213 pp.

Binder, A. B., R. E. Arvidson, E. A. Guinness, K. L. Jones, E. C. Morris, T. A. Mutch, D. C. Pieri, and C. Sagan (1977), The geology of the Viking Lander 1 site, *J. Geophys. Res.*, *82*, 4439–4451, doi:10.1029/JS082i028p04439.

Blong, R. J. (1970), The development of discontinuous gulles in a pumice catchment, *Am. J. Sci.*, *268*, 369–383, doi:10.2475/ajs.268.4.369.

Bouley, S., R. A. Craddock, N. Mangold, and V. Ansan (2010), Characterization of fluvial activity in Parana Valles using different age-dating techniques, *Icarus*, *207*, 686–698, doi:10.1016/j.icarus.2009.12.030.

Bray, D. I. (1979), Estimating average velocity in gravel-bed rivers, *J. Hydraul. Div. Am. Soc. Civ. Eng.*, *105*, 1103–1122.

Brice, J. C. (1966), Erosion and deposition in the loess-mantled Great Plains, Medicine Creek drainage basin, Nebraska, *U.S. Geol. Surv. Prof. Pap.*, *352-H*, 255–339.

Brownlie, W. R. (1981), Prediction of flow depth and sediment discharge in open channels, *Rep. no. KH-R-43A*, 232 pp., W.M. Keck Lab. of Hydraul. and Water Resour.,Calif. Inst. of Technol., Pasadena.

Carr, M. H. (1973), Volcanism on Mars, *J. Geophys. Res.*, *78*, 4049–4062, doi:10.1029/JB078i020p04049.

Carr, M. H. (1996), *Water on Mars*, 229 pp., Oxford Univ. Press, New York.

Carr, M. H. (2006), *The Surface of Mars*, 307 pp., Cambridge Univ. Press, Cambridge, U. K.

Carr, M. H., and F. C. Chuang (1997), Martian drainage densities, *J. Geophys. Res.*, *102*, 9145–9152, doi:10.1029/97JE00113.

Chu, P.-S., A. J. Nash, and F.-Y. Porter (1993), Diagnostic studies of two contrasting rainfall episodes in Hawaii: Dry 1981 and wet 1982, *J. Clim.*, *6*, 1457–1462, doi:10.1175/1520-0442(1993)006<1457:DSOTCR>2.0.CO;2.

Church, M. (1978), Palaeohydrological reconstructions from a Holocene valley fill, in *Fluvial Sedimentology*, edited by A. D. Miall, pp. 743–772, Can. Soc. of Pet. Geol., Calgary, Alberta, Canada.

Colaprete, A., and O. B. Toon (2003), Carbon dioxide clouds in an early dense Martian atmosphere, *J. Geophys. Res.*, *108*(E4), 5025, doi:10.1029/2002JE001967.

Collins, W. D., et al. (2004), Description of the NCAR Community Atmosphere Model (CAM 3.0), *Tech. Note NCAR/TN-464+STR*, 214 pp., Natl. Cent. for Atmos. Res., Boulder, Colo.

Craddock, R. A., and A. D. Howard (2002), The case for rainfall on a warm, wet early Mars, *J. Geophys. Res.*, *107*(E11), 5111, doi:10.1029/2001JE001505.

Craddock, R. A., and T. A. Maxwell (1993), Geomorphic evolution of the Martian highlands through ancient fluvial process, *J. Geophys. Res.*, *98*, 3453–3468, doi:10.1029/92JE02508.

Craddock, R. A., T. A. Maxwell, and A. D. Howard (1997), Crater morphometry and modification in the Sinus Sabaeus and Margaritifer Sinus regions of Mars, *J. Geophys. Res.*, *102*, 13,321–13,340, doi:10.1029/97JE01084.

Decker, R. W., and R. L. Christiansen (1984), Explosive eruptions of Kīlauea volcano, Hawaii, in *Explosive Volcanism: Inception, Evolution, and Hazards*, pp. 122–132, Natl. Acad. Press, Washington, D. C.

Dzurisin, D., J. P. Lockwood, T. J. Casadevall, and M. Rubin (1995), The Uwekahuna ash member of the Puna Basalt: Product of violent phreatomagmatic eruptions at Kīlauea volcano, Hawaii between 2800 and 2100 14C years ago, *J. Volcanol. Geotherm. Res.*, *66*, 163–184, doi:10.1016/0377-0273(94)00062-L.

Easton, R. M. (1987), Stratigraphy of Kīlauea Volcano, *U.S. Geol. Surv. Prof. Pap.*, *1350*, 243–260.

Edgett, K. S., and M. C. Malin (2000), New views of Mars eolian activity, materials, and surface properties: Three vignettes from the Mars Global Surveyor Mars Orbiter Camera, *J. Geophys. Res.*, *105*, 1623–1650.

Edgett, K. S., and M. C. Malin (2002), Martian sedimentary rock stratigraphy: Outcrops and interbedded craters of northwest Sinus Meridiani and southwest Arabia Terra, *Geophys. Res. Lett.*, *29*(24), 2179, doi:10.1029/2002GL016515.

Einstein, H. A. (1950), The bed-load function for sediment transportation in open channel flows, *Tech. Bull. 1026*, U.S. Dep. of Agric., Washington, D. C.

Elias, T., A. J. Sutton, J. B. Stokes, and T. J. Casadevall (1998), Sulfure dioxide emissions rates of Kīlauea Volcano, Hawaii, 1979–1997, *U.S. Geol. Surv. Open File Rep. 98–462*, 41 pp.

Fagents, S. A., and L. Wilson (1996), Numerical modelling of ejecta dispersal from transient volcanic explosions on Mars, *Icarus*, *123*, 284–295, doi:10.1006/icar.1996.0158.

Fanale, F. P., and W. A. Cannon (1971), Adsorption on the Martian regolith: Implications for the Martian volatile budget and diurnal brightening, *Nature*, *230*, 502–504, doi:10.1038/230502a0.

Fassett, C. I., and J. W. Head III (2008a), The timing of Martian valley network activity: Constraints from buffered crater counting, *Icarus*, *195*, 61–89, doi:10.1016/j.icarus.2007.12.009.

Fassett, C. I., and J. W. Head III (2008b), Valley network-fed, open-basin lakes on Mars: Distribution and implications for Noachian surface and subsurface hydrology, *Icarus*, *198*, 37–56, doi:10.1016/j.icarus.2008.06.016.

Fiske, R. S., T. R. Rose, D. A. Swanson, D. E. Champion, and J. P. McGeehin (2009), Kulanaokuaiki tephra (ca. A.D. 400–1000): Newly recognized evidence for highly explosive eruptions at Kīlauea Volcano, Hawai'i, *Geol. Soc. Am. Bull.*, *121*, 712–728, doi:10.1130/B26327.1.

Forget, F., and R. T. Pierrehumbert (1997), Warming early Mars with carbon dioxide clouds that scattered infrared radiation, *Science*, *278*, 1273–1276, doi:10.1126/science.278.5341.1273.

Freeze, R. A., and J. A. Cherry (1979), *Groundwater*, 604 pp., Prentice-Hall, Englewood Cliffs, N. J.

Gellert, R., et al. (2004), Chemistry of rocks and soils in Gusev Crater from the Alpha Particle X-ray Spectrometer, *Science*, *305*, 829–832, doi:10.1126/science.1099913.

Giambelluca, T., and M. Sanderson (1993), The water balance and climatic classification, in *Prevailing Trade Winds, Weather and Climate in Hawai'i*, edited by M. Sanderson, chap. 4, pp. 56–72, Univ. of Hawaii Press, Honolulu.

Goldspiel, J. M., S. W. Squyres, and D. G. Jankowski (1993), Topography of small Martian valleys, *Icarus*, *105*, 479–500, doi:10.1006/icar.1993.1143.

Gough, D. O. (1981), Solar interior structure and luminosity variations, *Solar Phys.*, *74*, 21–34.

Gulick, V. C. (2001), Origin of the valley networks on Mars: A hydrological perspective, *Geomorphology*, *37*, 241–268, doi:10.1016/S0169-555X(00)00086-6.

Harrison, K. P., and R. E. Grimm (2005), Groundwater-controlled valley networks and the decline of surface runoff on Early Mars, *J. Geophys. Res.*, *110*, E12S16, doi:10.1029/2005JE002455.

Head, J. W., III, and L. Wilson (2002), Mars: A review and synthesis of general environments and geological settings of magma-H_2O interactions, *Geol. Soc. Spec. Publ.*, *202*, 27–57, doi:10.1144/GSL.SP.2002.202.01.03.

Head, J. W., III, H. Hiesinger, M. A. Ivanov, M. A. Kreslavsky, S. Pratt, and B. J. Thomson (1999), Possible ancient oceans on Mars: Evidence from Mars Orbiter Laser Altimeter data, *Science*, *286*, 2134–2137, doi:10.1126/science.286.5447.2134.

Hey, R. D. (1979), Flow resistance in gravel-bed rivers, *J. Hydraul. Div. Am. Soc. Civ. Eng.*, *105*(4), 365–379.

Hoke, M. R. T., and B. M. Hynek (2009), Roaming zones of precipitation on ancient Mars as recorded in valley networks, *J. Geophys. Res.*, *114*, E08002, doi:10.1029/2008JE003247.

Horton, R. E. (1933), The role of infiltration in the hydrologic cycle, *Eos Trans. AGU*, *14*, 446–460.

Howard, A. D., W. E. Dietrich, and M. A. Seidl (1994), Modelling fluvial erosion on regional to continental scales, *J. Geophys. Res.*, *99*, 13,971–13,986, doi:10.1029/94JB00744.

Howard, A. D., J. M. Moore, and R. P. Irwin III (2005), An intense terminal epoch of widespread fluvial activity on early Mars: 1. Valley network incision and associated deposits, *J. Geophys. Res.*, *110*, E12S14, doi:10.1029/2005JE002459.

Hynek, B. M., M. Beach, and M. R. T. Hoke (2010), Updated global map of Martian valley networks and implications for climate and hydrologic processes, *J. Geophys. Res.*, *115*, E09008, doi:10.1029/2009JE003548.

Irwin, R. P., III, and A. D. Howard (2002), Drainage basin evolution in Noachian Terra Cimmeria, Mars, *J. Geophys. Res.*, *107*(E7), 5056, doi:10.1029/2001JE001818.

Irwin, R. P., III, A. D. Howard, R. A. Craddock, and J. M. Moore (2005a), An intense terminal epoch of widespread fluvial activity on early Mars: 2. Increased runoff and paleolake development, *J. Geophys. Res.*, *110*, E12S15, doi:10.1029/2005JE002460.

Irwin, R. P., III, R. A. Craddock, and A. D. Howard (2005b), Interior channels in Martian valley networks: Discharge and runoff production, *Geology*, *33*(6), 489–492, doi:10.1130/G21333.1.

Irwin, R. P., III, C. M. Fortezzo, S. Tooth, A. D. Howard, J. R. Zimbelman, C. J. Barnhart, A. J. Benthem, C. C. Brown, and R. A. Parsons (2009), Origin of theater-headed tributaries to Escalante and Glen Canyons, Utah, *Lunar Planet. Sci.*, *XL*, Abstract 1644.

Irwin, R. P., III, R. A. Craddock, A. D. Howard, and H. L. Flemming (2011), Topographic influences on development of Martian valley networks, *J. Geophys. Res.*, *116*, E02005, doi:10.1029/2010JE003620.

Ivanov, M. A., and J. W. Head (2006), Alba Patera, Mars: Topography, structure, and evolution of a unique late Hesperian–early Amazonian shield volcano, *J. Geophys. Res.*, *111*, E09003, doi:10.1029/2005JE002469.

Kereszturi, A. (2005), Cross-sectional and longitudinal profiles of valleys and channels in Xanthe Terra on Mars, *J. Geophys. Res.*, *110*, E12S17, doi:10.1029/2005JE002454.

Kleinhans, M. G. (2005), Flow discharge and sediment transport models for estimating minimum timescale of hydrological activity and channel and delta formation on Mars, *J. Geophys. Res.*, *110*, E12003, doi:10.1029/2005JE002521.

Komar, P. D. (1979), Comparisons of the hydraulics of water flows in Martian outflow channels with flows of similar scale on Earth, *Icarus*, *37*, 156–181, doi:10.1016/0019-1035(79)90123-4.

Komar, P. D. (1980), Modes of sediment transport in channelized water flows with ramifications to the erosion of the Martian outflow channels, *Icarus*, *42*, 317–329, doi:10.1016/0019-1035(80)90097-4.

Komar, P. D. (1988), Sediment transport by floods, in *Flood Geomorphology*, edited by V. R. Baker, R. C. Kochel, and P. C. Patton, pp. 97–111, Wiley-Intersci., New York.

Komatsu, G., and V. R. Baker (1997), Paleohydrology and flood geomorphology of Ares Vallis, *J. Geophys. Res.*, *102*(E2), 4151–4160, doi:10.1029/96JE02564.

Laity, J. E., and M. C. Malin (1985), Sapping processes and the development of theatre-headed valley networks on the Colorado Plateau, *Geol. Soc. Am. Bull.*, *96*, 203–217, doi:10.1130/0016-7606(1985)96<203:SPATDO>2.0.CO;2.

Lamb, M. P., A. D. Howard, J. Johnson, K. X. Whipple, W. E. Dietrich, and J. T. Perron (2006), Can springs cut canyons into rock?, *J. Geophys. Res.*, *111*, E07002, doi:10.1029/2005JE002663.

Leopold, L. B., and W. W. Emmett (1997), Bedload and river hydraulics: Inferences from the East Fork River, Wyoming, *U.S. Geol. Surv. Prof. Paper 1583*, 52 pp.

Leopold, L. B., M. G. Wolman, and J. P. Miller (1992), *Fluvial Processes in Geomorphology*, 522 pp., Dover, Mineola, New York.

Limerinos, J. T. (1970), Determination of the Manning coefficient from measured bed roughness in natural channels, *U.S. Geol. Surv. Water Supply Pap.*, *1898B*, 47 pp.

Liu, H. K., and S. Y. Hwang (1959), Discharge formula for straight alluvial channels, *J. Hydraul. Div. Am. Soc. Civ. Eng.*, *85*, 65–97.

Luo, W., and T. F. Stepinski (2009), Computer-generated global map of valley networks on Mars, *J. Geophys. Res.*, *114*, E11010, doi:10.1029/2009JE003357.

Mabbutt, J. A. (1977), *Desert Landforms*, 340 pp., Aust. Natl. Univ. Press, Canberra.

Malin, M. C., and K. S. Edgett (2000), Sedimentary rocks of early Mars, *Science*, *290*, 1927–1937, doi:10.1126/science.290.5498.1927.

Malin, M. C., and K. S. Edgett (2001), Mars Global Surveyor Mars Orbiter Camera: Interplanetary cruise through primary mission, *J. Geophys. Res.*, *106*, 23,429–23,570, doi:10.1029/2000JE001455.

Malin, M. C., D. Dzurisin, and R. P. Sharp (1983), Stripping of Keanakakoi tephra on Kīlauea Volcano, Hawaii, *Geol. Soc. Am. Bull.*, *94*, 1148–1158, doi:10.1130/0016-7606(1983)94<1148:SOKTOK>2.0.CO;2.

Manga, M., A. Patel, J. Dufek, and E. S. Kite (2012), Wet surface and dense atmosphere on early Mars suggested by the bomb sag at Home Plate, Mars, *Geophys. Res. Lett.*, *39*, L01202, doi:10.1029/2011GL050192.

Mangold, N., C. Quantin, V. Ansan, C. Delacourt, and P. Allemand (2004), Evidence for precipitation on Mars from dendritic valleys in the Valles Marineris area, *Science*, *305*(5680), 78–81, doi:10.1126/science.1097549.

Mangold, N., S. Adeli, S. Conway, V. Ansan, and B. Langlais (2012), A chronology of early Mars climatic evolution from impact crater degradation, *J. Geophys. Res.*, *117*, E04003, doi:10.1029/2011JE004005.

Mastin, L. G. (1997), Evidence for water influx from a caldera lake during the explosive hydromagmatic eruption of 1790, Kīlauea volcano, Hawaii, *J. Geophys. Res.*, *102*, 20,093–20,109, doi:10.1029/97JB01426.

Masursky, H., J. M. Boyce, A. L. Dial, G. G. Schaber, and M. E. Strobell (1977), Classification and time of formation of Martian channels based on Viking data, *J. Geophys. Res.*, *82*, 4016–4038, doi:10.1029/JS082i028p04016.

McPhie, J., G. P. L. Walker, and R. L. Christiansen (1990), Phreatomagmatic and phreatic fall and surge deposits from explosions at Kīlauea volcano, Hawaii, 1790 A.D.: Keanakakoi ash member, *Bull. Volcanol.*, *52*, 334–354, doi:10.1007/BF00302047.

McSween, H. Y. (1994), What we have learned about Mars from SNC meteorites, *Meteoritics*, *29*, 757–779, doi:10.1111/j.1945-5100.1994.tb01092.x.

Meigs, P. (1953), World distribution of arid and semi-arid homoclimates, in *Reviews of Research on Arid Zone Hydrology*, pp. 203–209, U. N. Educ. Sci. and Cult. Org., Paris.

Mest, S. C., and D. A. Crown (2008), Comparison of mapped and modeled watersheds in the Tyrrhena Terra region of Mars, in *Second Workshop on Mars Valley Networks*, pp. 55–58, Smithsonian Inst., Washington, D. C.

Mest, S. C., D. A. Crown, and W. Harbert (2010), Watershed modeling in the Tyrrhena Terra region of Mars, *J. Geophys. Res.*, *115*, E09001, doi:10.1029/2009JE003429.

Meyer-Peter, E., and R. Müller (1948), Formulas for bed-load transport, in *Proceedings of the 2nd Meeting of the International Association for Hydraulic Structures Research*, pp. 39–64, Int. Assoc. for Hydraul. Res., Stockholm.

Mutch, T. A., R. A. Arvidson, A. B. Binder, E. A. Guinness, and E. C. Morris (1977), The geology of the Viking Lander 2 site, *J. Geophys. Res.*, *82*, 4452–4467, doi:10.1029/JS082i028p04452.

Neal, C. A., and J. P. Lockwood (2003), Geologic map of the summit region of Kīlauea Volcano, Hawaii, *U.S. Geol. Surv. Geol. Invest. Ser. Map*, *I-2759*, scale 1:24,000.

Parker, T. J., R. S. Saunders, and D. M. Schneeberger (1989), Transitional morphology in west Deuteronilus Mensae, Mars: Implications for modification of the lowland/upland boundary, *Icarus*, *82*, 111–145, doi:10.1016/0019-1035(89)90027-4.

Pieri, D. C. (1980), Martian valleys: Morphology, distribution, age, and origin, *Science*, *210*, 895–897, doi:10.1126/science.210.4472.895.

Powers, H. A. (1948), A chronology of the explosive eruptions of Kīlauea, *Pac. Sci.*, *2*, 278–292.

Powers, S. (1916), Explosive ejectament of Kīlauea, *Am. J. Sci.*, *41*, 227–244.

Quantin, C., and R. A. Craddock (2008), Timing of Martian Valley Network using fine scale age determination, paper presented at Second Workshop on Mars Valley Networks, Smithsonian Inst., Moab, Utah.

Ramage, C. S. (1962), The subtropical cyclone, *J. Geophys. Res.*, *67*, 1401–1411, doi:10.1029/JZ067i004p01401.

Raudkivi, A. J. (1967), *Loose Boundary Hydraulics*, 331 pp., Pergamon, Oxford, U. K.

Reid, I., and L. E. Frostick (2011), Channel form, flows and sediments in deserts, in *Arid Zone Geomorphology: Process, Form and Change in Drylands*, edited by D. S. G. Thomas, pp. 205–229, John Wiley, New York, doi:10.1002/9780470710777.ch13.

Richardson, M. I., and M. Soto (2008), Controls on precipitation and aridity for ancient Mars, paper presented at Second Workshop on Mars Valley Networks, Smithsonian Inst., Moab, Utah.

Sagan, C., and G. Mullen (1972), Earth and Mars: Evolution of atmospheres and surface temperatures, *Science*, *177*, 52–56, doi:10.1126/science.177.4043.52.

Schiffman, P., R. Zierenberg, N. Marks, J. L. Bishop, and M. D. Dyar (2006), Acid-fog deposition at Kīlauea volcano: A possible mechanism for the formation of siliceous-sulfate rock coatings on Mars, *Geology*, *34*, 921–924, doi:10.1130/G22620A.1.

Selby, M. J. (1993), *Hillslope Materials and Processes*, 451 pp., Oxford Univ. Press, Oxford, U. K.

Shields, A. (1936), Application of similarity principles and turbulence research to bed load movement, 26 pp., U.S. Dep. of Agric., Soil Conserv. Serv. Coop. Lab., Calif. Inst. of Technol., Pasadena.

Silberman, E., R. W. Carter, H. A. Einstein, J. Hinds, and R. W. Powell (1963), Friction factors in open channels: Progress report of the task force on friction factors in open channels of the Committee of Hydromechanics of the Hydraulics Division, *J. Hydraul. Div. Am. Soc. Civ. Eng.*, *89*, 97–143.

Soderblom, L. A., T. J. Kreidler, and H. Masursky (1973), Latitudinal distribution of a debris mantle on the Martian surface, *J. Geophys. Res.*, *78*, 4117–4122, doi:10.1029/JB078i020p04117.

Soto, A., M. I. Richardson, and C. E. Newman (2010), Global constraints on rainfall on ancient Mars: Oceans, lakes, and valley networks, *Lunar Planet. Sci.*, *XLI*, Abstract 2397.

Squyres, S. W., and J. F. Kasting (1994), Early Mars: How warm and how wet?, *Science*, *265*, 744–749, doi:10.1126/science.265.5173.744.

Squyres, S. W., et al. (2004), The Spirit Rover's Athena Science Investigation at Gusev Crater, Mars, *Science*, *305*, 794–799, doi:10.1126/science.3050794.

Squyres, S. W., et al. (2007), Pyroclastic activity at Home Plate in Gusev Crater, Mars, *Science*, *316*, 738–742, doi:10.1126/science.1139045.

Stearns, H. T., and G. A. MacDonald (1946), Geology and groundwater resources of the Island of Hawaii, *Bull. 9*, 363 pp., Hawaii Div. of Hydrogr., U.S. Geol. Surv., Honolulu.

Stocking, M. A. (1980), Examination of the factors controlling gully growth, in *Assessment of Erosion*, edited by M. D. Boodt and D. Gabriels, pp. 505–520, John Wiley, Hoboken, N. J.

Stone, J. B. (1926), *The Products and Structure of Kīlauea*, vol. 33, 60 pp., B.P. Bishop Honolulu.

Swanson, D. A., and R. L. Christiansen (1973), Tragic base surge in 1790 at Kīlauea Volcano, *Geology*, *1*, 83–86, doi:10.1130/0091-7613(1973)1<83:TBSIAK>2.0.CO;2.

Swanson, D. A., J. P. McGeehin, T. R. Rose, and R. S. Fiske (2004), Age of the Keanakāko'i Ash, Kīlauea Volcano, *Eos Trans. AGU*, *85*(28), West. Pac. Geophys. Meet. Suppl., Abstract V33A-88.

Swanson, D. A., T. R. Rose, R. S. Fiske, and J. P. McGeehin (2012), Keanakāko'i tephra produced by 300 years of explosive eruptions following collapse of Kīlauea's caldera in about 1500 CE, *J. Volcanol. Geotherm. Res.*, *215–216*, 8–25, doi:10.1016/j.jvolgeores.2011.11.009.

Thome, C. R., and L. W. Zevenbergen (1985), Estimating mean velocity in mountain rivers, *J. Hydraul. Eng. Am. Soc. Civ. Eng.*, *111*, 612–624, doi:10.1061/(ASCE)0733-9429(1985)111:4(612).

Wentworth, C. K. (1938), Ash formations on the Island of Hawaii, *Hawaiian Volcano Observ. Spec. Rep. 3*, 183 pp., Hawaii Volcano Res. Assoc., Honolulu.

White, S. J. (1970), Plane bed thresholds of fine-grained sediments, *Nature*, *228*, 152–153, doi:10.1038/228152a0.

Williams, R. M. E., and M. C. Malin (2004), Evidence for late stage fluvial activity in Kasei Valles, Mars, *J. Geophys. Res.*, *109*, E06001, doi:10.1029/2003JE002178.

Williams, R. M. E., and R. J. Phillips (2001), Morphometric measurements of Martian valley networks from Mars Orbiter Laser Altimeter (MOLA) data, *J. Geophys. Res.*, *106*, 23,737–23,752.

Wilson, L. (1999), Explosive Volcanic Eruptions X: The influence of pyroclast size distributions and released magma gas contents on the eruption velocities of pyroclasts and gas in Hawaiian and Plinian eruptions, *Geophys. J. Int.*, *136*, 609–619, doi:10.1046/j.1365-246x.1999.00750.x.

Wilson, D., T. Elias, T. Orr, M. Patrick, J. Sutton, and D. Swanson (2008), Small explosion from New Vent at Kīlauea's summit, *Eos Trans. AGU*, *89*(22), 203, doi:10.1029/2008EO220003.

Wilson, L., and J. W. Head (2004), Evidence for a massive phreatomagmatic eruption in the initial stages of formation of the Mangala Valles outflow channel, Mars, *Geophys. Res. Lett.*, *31*, L15701, doi:10.1029/2004GL020322.

Wilson, L., and P. J. Mouginis-Mark (2003), Phreatomagmatic explosive activity at Hrad Vallis, Mars, *J. Geophys. Res.*, *108*(E8), 5082, doi:10.1029/2002JE001927.

Woolfe, K. J., and R. G. Purdon (1996), Deposits of a rapidly eroding meandering river: Terrace cut and fill in the Taupo Volcanic Zone, *N.Z. J. Geol. Geophys.*, *39*, 243–249, doi:10.1080/00288306.1996.9514708.

Yalin, M. S. (1977), *Mechanics of Sediment Transport*, 288 pp., Pergamon, New York.

Zablocki, C. J., R. I. Tilling, D. W. Peterson, R. I. Christiansen, G. V. Keller, and J. C. Murray (1974), A deep research drill hole at the summit of an active volcano, Kīlauea, Hawaii, *Geophys. Res. Lett.*, *1*, 323–326, doi:10.1029/GL001i007p00323.

Zhang, R. (1997), Determination of soil sorptivity and hydraulic conductivity from the disk infiltrometer, *Soil Sci. Soc. Am. J.*, *61*(4), 1024–1030, doi:10.2136/sssaj1997.03615995006100040005x.